

# Open Research Online

---

The Open University's repository of research publications and other research outputs

## Soil, senescence and exudate utilisation: characterisation of the Paragon var. spring bread wheat root microbiome

### Journal Item

How to cite:

Prudence, Samuel MM.; Newitt, Jake T.; Worsley, Sarah F.; Macey, Michael C.; Murrell, J. Colin; Lehtovirta-Morley, Laura E. and Hutchings, Matthew I. (2021). Soil, senescence and exudate utilisation: characterisation of the Paragon var. spring bread wheat root microbiome. *Environmental Microbiome*, 16(1), article no. 12.

For guidance on citations see [FAQs](#).

© 2021 Samuel MM. Prudence et al.



<https://creativecommons.org/licenses/by/4.0/>

Version: Version of Record

Link(s) to article on publisher's website:

<http://dx.doi.org/doi:10.1186/s40793-021-00381-2>

---

Copyright and Moral Rights for the articles on this site are retained by the individual authors and/or other copyright owners. For more information on Open Research Online's data [policy](#) on reuse of materials please consult the policies page.

---

RESEARCH ARTICLE

Open Access



# Soil, senescence and exudate utilisation: characterisation of the Paragon var. spring bread wheat root microbiome

Samuel MM. Prudence<sup>1\*†</sup> , Jake T. Newitt<sup>†1</sup>, Sarah F. Worsley<sup>2</sup>, Michael C. Macey<sup>3</sup>, J. Colin Murrell<sup>4</sup>, Laura E. Lehtovirta-Morley<sup>2\*</sup> and Matthew I. Hutchings<sup>1\*</sup>

## Abstract

**Background:** Conventional methods of agricultural pest control and crop fertilisation are unsustainable. To meet growing demand, we must find ecologically responsible means to control disease and promote crop yields. The root-associated microbiome can aid plants with disease suppression, abiotic stress relief, and nutrient bioavailability. The aim of the present work was to profile the community of bacteria, fungi, and archaea associated with the wheat rhizosphere and root endosphere in different conditions. We also aimed to use <sup>13</sup>C<sub>2</sub>O<sub>2</sub> stable isotope probing (SIP) to identify microbes within the root compartments that were capable of utilising host-derived carbon.

**Results:** Metabarcoding revealed that community composition shifted significantly for bacteria, fungi, and archaea across compartments. This shift was most pronounced for bacteria and fungi, while we observed weaker selection on the ammonia oxidising archaea-dominated archaeal community. Across multiple soil types we found that soil inoculum was a significant driver of endosphere community composition, however, several bacterial families were identified as core enriched taxa in all soil conditions. The most abundant of these were *Streptomycetaceae* and *Burkholderiaceae*. Moreover, as the plants senesce, both families were reduced in abundance, indicating that input from the living plant was required to maintain their abundance in the endosphere. Stable isotope probing showed that bacterial taxa within the *Burkholderiaceae* family, among other core enriched taxa such as *Pseudomonadaceae*, were able to use root exudates, but *Streptomycetaceae* were not.

**Conclusions:** The consistent enrichment of *Streptomycetaceae* and *Burkholderiaceae* within the endosphere, and their reduced abundance after developmental senescence, indicated a significant role for these families within the wheat root microbiome. While *Streptomycetaceae* did not utilise root exudates in the rhizosphere, we provide evidence that *Pseudomonadaceae* and *Burkholderiaceae* family taxa are recruited to the wheat root community via root exudates. This deeper understanding crop microbiome formation will enable researchers to characterise these interactions further, and possibly contribute to ecologically responsible methods for yield improvement and biocontrol in the future.

**Keywords:** Wheat, Exudate, Root, Microbiome, Senescence, Endosphere, Streptomyces, Archaea, Isotope, Metabarcoding

\* Correspondence: [sam.prudence@jic.ac.uk](mailto:sam.prudence@jic.ac.uk); [l.lehtovirta-morley@uea.ac.uk](mailto:l.lehtovirta-morley@uea.ac.uk); [matt.hutchings@jic.ac.uk](mailto:matt.hutchings@jic.ac.uk)

<sup>†</sup>Samuel MM. Prudence and Jake T. Newitt contributed equally to this work.

<sup>1</sup>Department of Molecular Microbiology, John Innes Centre, Norwich Research Park, Norwich NR4 7UH, UK

<sup>2</sup>School of Biological Sciences, University of East Anglia, Norwich Research Park, Norwich NR4 7TJ, UK

Full list of author information is available at the end of the article



© The Author(s). 2021 **Open Access** This article is licensed under a Creative Commons Attribution 4.0 International License, which permits use, sharing, adaptation, distribution and reproduction in any medium or format, as long as you give appropriate credit to the original author(s) and the source, provide a link to the Creative Commons licence, and indicate if changes were made. The images or other third party material in this article are included in the article's Creative Commons licence, unless indicated otherwise in a credit line to the material. If material is not included in the article's Creative Commons licence and your intended use is not permitted by statutory regulation or exceeds the permitted use, you will need to obtain permission directly from the copyright holder. To view a copy of this licence, visit <http://creativecommons.org/licenses/by/4.0/>. The Creative Commons Public Domain Dedication waiver (<http://creativecommons.org/publicdomain/zero/1.0/>) applies to the data made available in this article, unless otherwise stated in a credit line to the data.

## Background

Wheat is a staple crop for more than 4 billion people and globally accounts for more than 20% of human caloric and protein consumption [1]. This means that farming wheat, and the accompanying use of chemical fertilisers and pesticides, has a huge environmental

impact worldwide. For example, up to 70% of nitrogen fertiliser is lost each year through run-off and microbial denitrification which generates the potent greenhouse gas  $N_2O$  [2]. The challenge facing humans this century is to grow enough wheat to feed an increasing global human population while reducing our reliance on agrochemicals which contribute to climate change and damage ecosystems [3]. One possible way to achieve this is to manipulate the microbial communities associated with wheat and other crop plants. These communities are commonly referred to as “microbiomes” and a healthy microbiome can enhance host fitness by providing essential nutrients [4], increasing resilience to abiotic stressors [5], and protecting against disease [4]. Each new generation of plants must recruit the microbial species (archaea, bacteria, fungi and other micro-eukarya) that make up its root microbiome from the surrounding soil, and this means that the soil microbial community is an important determinant of plant root microbiome composition [6].

Plants are able to influence the microbial community in the rhizosphere, which is the soil most closely associated with the roots, and the endosphere, which is the inside of the roots. The microbes within these root-associated environments tend to have traits which benefit the host plant [7] and plants modulate these microbial communities by depositing photosynthetically fixed carbon into the rhizosphere in the form of root exudates, a complex mixture of organic compounds consisting primarily of sugars, organic acids, and fatty acids [8]. Plants deposit up to 40% of their fixed carbon into the soil [9], and there is evidence to suggest that certain molecules within these exudates can attract specific bacterial taxa [6, 10, 11]. Thus, the implication is that host plants attract specific microbial taxa from a diverse microbial soil community, and generate a root microbiome that contains only the subset of the soil community most likely to offer benefits to the host plant [12]. In return, the growth of beneficial microbes is supported by the nutrients from root exudates, such that the plants and microbes exchange resources in a mutually beneficial symbiosis. Traditional plant breeding may have had a negative effect on this process in important food crops such as barley and wheat; for example, selection for traits such as increased growth and yield may have inadvertently had a negative influence on root exudation and microbiome formation [8, 11]. Long-term use of fertilizer also reduces the dependency of the host plant on microbial interactions, further weakening the selective pressure to maintain costly exudation of root metabolites [13]. This highlights the need for a greater understanding of the factors that underpin microbiome assembly and function in important domesticated crop species such as bread wheat, *Triticum aestivum*.

To understand the key functions in a host-associated microbial community, it can be useful to define the core microbiome, i.e. the microbial taxa consistently associated with a particular plant species regardless of habitat or conditions, and which provide a service to the host plant and/or the broader ecosystem [14, 15]. The core microbiome of the model plant *Arabidopsis thaliana* is well studied [6, 16], and it has also been characterized for numerous other plant species to varying degrees [17–19]. In elucidating the core microbiome a number of factors must be accounted for, including soil type [20, 21], developmental stage [22, 23], genotype [8, 22, 24] and, in the case of crop plants, agricultural management strategy [23, 25–27]. The core microbiome has been investigated for bread wheat [28–32] and, while most studies focus on the rhizosphere, Kuźniar *et al.* [28] identified a number of core bacterial genera within the endosphere including *Pseudomonas* and *Flavobacterium*. Their study focussed on a single soil type and developmental stage, but to reliably identify the core microbial taxa associated with wheat, more of the aforementioned factors must be analysed. Microbial community surveys are also often limited to investigations of bacterial or, in some cases, fungal diversity meaning that knowledge of wheat root community diversity is limited to these two groups. Root-associated archaea are considerably understudied, particularly within terrestrial plant species such as wheat. Most generic and commonly used 16S rRNA gene PCR primer sets fail to capture archaeal diversity [33], thus the diversity of archaea within soils is commonly overlooked. Key soil groups such as ammonia oxidizing archaea (AOA) play a significant role in nitrogen cycling, a key ecological service, and one study has managed to link an AOA to plant beneficial traits [34], suggesting that the role of archaea within the terrestrial root associated microbiome warrants further study.

For many important crops such as wheat, barley, maize, corn, and rice, developmental senescence is a crucial determinant of yield and nutrient content [35, 36]. Developmental senescence occurs at the end of the life cycle, and during this process, resources, particularly nitrogen, are diverted from plant tissues into the developing grain [35, 36]. Senescence represents a dramatic shift in the metabolic activity of the plant [35] and in the regulation of pathways of pathogen defence [36, 37]. Given that root exudation is a dynamic process [38], it would be reasonable to assume that senescence affects root exudation substantially, particularly because of the diversion of nitrogen to the developing grain (several major wheat root exudate compounds, like amino acids, nucleosides, and numerous organic acids, contain nitrogen [38]). To our knowledge, changes within the wheat root microbial community during wheat senescence have not been investigated previously. Given the pivotal role

senescence plays in grain development and yields, microbial community dynamics during this process warrant investigation. At the onset of senescence, plant resources are redirected to the seed, root exudation is reduced, and root tissues start to decay. It is plausible that this shift in plant metabolism would cause a change in the root-associated microbiome, and greater understanding of this could inform agricultural management strategies and the design of new crop cultivars.

One major limitation of metabarcoding approaches is that they do not reveal which microbial taxa are actively interacting with plants, for example via the utilisation of compounds exuded by the roots.  $^{13}\text{C}$  DNA stable Isotope Probing (SIP) is a powerful tool, with significant potential for applications exploring the role of root exudates in microbiome assembly. As plants are incubated with  $^{13}\text{C}$ , the heavy carbon is fixed and incorporated into exuded organic compounds. Microbial communities that actively metabolise root exudates will incorporate  $^{13}\text{C}$  into their DNA and can thus be identified [9, 39]. Thus, DNA-SIP can be used to identify microbiota within the community which are capable of utilising host-derived carbon, then the importance of this capability for success within the root microbiome can be assessed. While numerous DNA-SIP studies have probed metabolically active communities associated with wheat, few have assessed root exudate metabolism directly using high-throughput sequencing methods for microbial identification [40, 41]. Of the two studies that have, similar findings were presented but with some distinct differences. Both studies showed that exudate-metabolising microbial communities in the rhizosphere consisted primarily of Actinobacteria and Proteobacteria [42, 43]. Taxa from Burkholderiales specifically were shown to dominate exudate metabolism in one study [42], whereas the other highlighted *Paenibacillaceae* as exudate metabolisers within the rhizosphere [43]. Discrepancies between these studies likely result from different soil types and wheat genotypes, and this demonstrates a need for further DNA-SIP experiments using different soils and different wheat varieties.

In this study we characterised the rhizosphere and endosphere microbiomes of *Triticum aestivum* variety Paragon, an UK elite spring bread wheat, using metabarcoding and  $^{13}\text{C}$  DNA-SIP. Although wheat rhizosphere bacterial communities have been well characterised under a wide range of conditions [22, 24, 29–31, 44], few studies have surveyed the endosphere community. Here, we profile the archaeal, bacterial and fungal communities in the bulk soil, rhizosphere and endosphere compartments of *T. aestivum* var. Paragon using 16S rRNA gene and ITS2 amplicon sequencing. We further characterise the bacterial communities using  $^{13}\text{C}$  DNA-SIP. We aimed to address the following questions: (1) Are there any core

microbial taxa within the endosphere and rhizosphere of *T. aestivum* var. Paragon across starkly contrasting soil environments? (2) How does the community change as the plant enters developmental senescence, and which microbial taxa, if any, are unable to persist through senescence? (3) Do wheat roots select for specific archaeal lineages as they do for bacteria and fungi? (4) Which bacterial taxa utilise wheat root exudates? The results provide a significant advance towards understanding wheat-microbiome interactions and establishing an understanding of the core microbial taxa in *T. aestivum* var. Paragon.

## Methods

### Soil sampling and chemical analyses

Agricultural soil was sampled in April 2019 from the John Innes Centre (JIC) Church Farm cereal crop research station in Bawburgh (Norfolk, United Kingdom) (52°37'39.4"N 1°10'42.2"E). The top 20 cm of soil was removed prior to sampling. Levington F2 compost was obtained from the John Innes Centre. Soil was stored at 4 °C and pre-homogenised prior to use. Chemical analysis was performed by the James Hutton Institute Soil Analysis Service (Aberdeen, UK) to measure soil pH, organic matter (%), and the phosphorus, potassium, and magnesium content (mg / kg) (Supplementary Table 3). To quantify inorganic nitrate and ammonium concentrations a KCl extraction was performed where 3 g of each soil type suspended in 24 ml of 1 M KCl in triplicate and incubated for 30 min with shaking at 250 rpm. To quantify ammonium concentration (g / kg) the colorimetric indophenol blue method was used [45]. For nitrate concentration (g / kg) vanadium (III) chloride reduction coupled to the colorimetric Griess reaction as previously described in Miranda *et al.* [46]. The agricultural soil was mildly alkaline (pH 7.97), contained only 2.3% organic matter and was relatively low in inorganic nitrogen, magnesium and potassium. Levington F2 compost was acidic (pH 4.98) and had a high organic matter content (91.1%) as well as higher levels of inorganic nitrogen, phosphorus, potassium and magnesium (Supplementary Table 3).

### Wheat cultivation, sampling and DNA extraction

For field-based experiments triplicate Paragon var. *Triticum aestivum* plants were sampled during the stem elongation growth phase approximately 200 days after sowing, in July 2019. To assess microbial diversity after senescence, triplicate Paragon var. *T. aestivum* plants were sampled immediately before harvest in August 2020 approximately 230 days after sowing. All field grown plants were sampled from the JIC Church Farm field studies site in Bawburgh (Norfolk, United Kingdom) (52°37'42.0"N 1°10'36.3"E) and were cultivated in the same field from which agricultural soil was sampled.

One bulk soil sample was taken during each sampling trip, where a sterile 50 ml falcon tube was filled with unplanted soil sampled approximately 30 cm away from the plant, in the same way as described for soil sampling. Bulk soil samples were snap-frozen and stored at  $-80^{\circ}\text{C}$  prior to triplicate DNA extractions.

For pot experiments Paragon var. *T. aestivum* seeds were soaked for 2 min in 70% ethanol (v/v), 10 min in 3% sodium hypochlorite (v/v) and washed 10 times with sterile water to sterilise the seed surface. Seeds were sown into pots of pre-homogenised Church farm agricultural soil, Levington F2 compost, or a 50:50 (v/v) mix of the two, in triplicate for each soil condition. Plants were propagated for 30 days at  $21^{\circ}\text{C}$  under a 12 h light / 12 h dark photoperiod before endosphere, rhizosphere and bulk soil samples were analysed. Then, for three plants per condition all three root compartments were sampled (Church farm agricultural soil, Levington F2 compost, 50:50 vol/vol mix). For each pot, after the plant was de-potted the soil was homogenised and a bulk soil sample was taken.

For all plants (both field and pot cultivated) first the phyllosphere was removed using a sterile scalpel and discarded prior to rhizosphere and endosphere sampling. Loose soil was then lightly shaken off of the roots, then roots were washed in phosphate buffered saline (PBS) (6.33 g  $\text{NaH}_2\text{PO}_4\cdot\text{H}_2\text{O}$ , 16.5 g  $\text{Na}_2\text{HPO}_4\cdot\text{H}_2\text{O}$ , 1 L  $\text{dH}_2\text{O}$ , 0.02% Silwett L-77 (v/v)). Pelleted material from this wash was analysed as the rhizosphere sample. To obtain the endosphere samples, remaining soil particles were washed off of the roots with PBS buffer. Then roots were soaked for 30 s in 70% ethanol (v/v), 5 min in 3% sodium hypochlorite (v/v) and washed 10 times with sterile water for surface sterilisation. To remove the rhizoplane roots were then sonicated for 20 min in a sonicating water bath [6]. After processing, all root, rhizosphere, and soil samples were snap-frozen and stored at  $-80^{\circ}\text{C}$ . The frozen root material was ground up in liquid nitrogen with a pestle and mortar. For all samples DNA was extracted using the FastDNA™ SPIN Kit for Soil (MP Biomedical) according to manufacturer's protocol with minor modifications: incubation in DNA matrix buffer was performed for 12 min and elution carried out using 75  $\mu\text{l}$  DNase/Pyrogen-Free Water. All DNA samples were stored at  $-20^{\circ}\text{C}$ . DNA quality and yields were assessed using a nanodrop and Qubit fluorimeter.

#### $^{13}\text{C}$ CO<sub>2</sub> labelling of wheat for DNA-SIP

Agricultural soil was sampled in July 2019, sampling method was as previously described. The soil was homogenized; any organic matter, or stones larger than ~ 3 cm, were removed before soil was spread out to a depth of ~ 2 cm and dried at  $20^{\circ}\text{C}$  overnight. Soil was added to pots and wetted before surface sterilized *T.*

*aestivum* var. Paragon seeds were sown (surface sterilisation performed as described above), three additional pots remained unplanted as controls for autotrophic CO<sub>2</sub> fixation by soil microorganisms. Plants were grown in unsealed gas tight 4.25 L PVC chambers under a 12 h light / 12 h dark photoperiod at  $21^{\circ}\text{C}$  for 3 weeks. Then at the start of each photoperiod the chambers were purged with CO<sub>2</sub> free air (80% nitrogen, 20% oxygen, British Oxygen Company, Guilford, UK) and sealed prior to pulse CO<sub>2</sub> injection every hour. During each photoperiod 3 plants and 3 unplanted soil controls were injected with  $^{13}\text{C}$  CO<sub>2</sub> (99% Cambridge isotopes, Massachusetts, USA) and 3 plants were injected with  $^{12}\text{C}$  CO<sub>2</sub>. Headspace CO<sub>2</sub> was maintained at 800ppmv (~twice atmospheric CO<sub>2</sub>). Plant CO<sub>2</sub> uptake rates were determined every 4 days to ensure the volume of CO<sub>2</sub> added at each 1 h interval would maintain approximately 800ppmv. For this, headspace CO<sub>2</sub> concentrations were measured using gas chromatography every hour. Measurements were conducted using an Agilent 7890A gas chromatography instrument, with flame ionization detector, a Poropak Q (6 ft.  $\times$  1/8") HP plotQ column (30 m  $\times$  0.530 mm, 40  $\mu\text{m}$  film), a nickel catalyst, and a helium carrier gas. The instrument ran with the following settings: injector temperature  $250^{\circ}\text{C}$ , detector temperature  $300^{\circ}\text{C}$ , column temperature  $115^{\circ}\text{C}$  and oven temperature  $50^{\circ}\text{C}$ . The injection volume was 100  $\mu\text{l}$  and run time was 5mins (CO<sub>2</sub> retention time is 3.4 mins). A standard curve was used to calculate CO<sub>2</sub> ppmv from peak areas. Standards of known CO<sub>2</sub> concentration were prepared in nitrogen flushed 120 ml serum vials. The volume of CO<sub>2</sub> injected at each 1 h interval to maintain 800ppmv CO<sub>2</sub> was calculated as follows:  $\text{Vol CO}_2 \text{ (ml)} = (800 \text{ (ppmv)} - \text{headspace CO}_2 \text{ after 1 h (ppmv)}) / 1000 * 4.25\text{(L)}$ . At the end of each photoperiod, tube lids were removed to prevent build-up of CO<sub>2</sub> during the dark period. At the start of the next 12 h, photoperiod tubes were flushed with CO<sub>2</sub> free air and headspace CO<sub>2</sub> was maintained at 800ppmv as described. After 14 days of labelling for all plants bulk soil, rhizosphere, and endosphere compartments were sampled as described previously and snap-frozen prior to DNA extraction as described previously.

#### Density gradient ultracentrifugation and fractionation for DNA-SIP

Density gradient ultracentrifugation was used to separate  $^{13}\text{C}$  labelled DNA from  $^{12}\text{C}$  DNA as previously described by Neufeld and colleagues [47]. Briefly, for each sample 700 ng of DNA was mixed with a 7.163 M CsCl solution and gradient buffer (0.1 M Tris-HCl pH 8, 0.1 M KCl, 1 mM EDTA) to a final measured buoyant density of  $1.725 \text{ g / ml}^{-1}$ . Buoyant density was determined via the refractive index using a refractometer (Reichert

Analytical Instruments, NY, USA). Samples were loaded into polyallomer quick seal centrifuge tubes (Beckman Coulter) and heat-sealed. Tubes were placed into a Vti 65.2 rotor (Beckman-Coulter) and centrifuged for 62 h at 44,100 rpm (~177,000 g) at 20 °C under a vacuum. Samples were fractionated by piercing the bottom of the ultracentrifuge tube with a 0.6 mm (23 gauge) sterile needle and dH<sub>2</sub>O was pumped into the centrifuge tube at a rate of 450 µl per minute, displacing the gradient into 1.5 ml microcentrifuge tubes. Fractions were collected until the water had fully displaced the gradient solution; this resulted in 12 450 µl fractions. The DNA was precipitated from fractions by adding 4 µl of Coprecipitant Pink Linear Polyacrylamide (Bioline) and 2 volumes of PEG-NaCl solution (30% w/v polyethylene glycol 6000, 1.6 M NaCl) to each fraction, followed by an overnight incubation at 4 °C. Fractions were then centrifuged at 21,130 g for 30 min and the supernatant was discarded. The DNA pellet was washed in 500 µl 70% EtOH and centrifuged at 21,130 g for 10 min. The resulting pellet was air-dried and resuspended in 30 µl sterile dH<sub>2</sub>O. Fractions were then stored at -20 °C. Fractions were pooled prior to sequencing (supplementary Table 4), sequencing was performed as described in the DNA sequencing and analysis section, except that peptide nucleic acid (PNA) blockers were used to prevent amplification of chloroplast and mitochondrial 16S rRNA genes.

#### Denaturing gradient gel electrophoresis (DGGE)

DGGE was performed separately on the bacterial and archaeal 16S rRNA genes to screen SIP fractions for a change in the community in the heavy compared to the light fractions, and between the <sup>13</sup>CO<sub>2</sub> labelled heavy fractions and those of the <sup>12</sup>CO<sub>2</sub> control plants. A nested PCR approach was taken to amplify the archaeal 16S rRNA gene, the first round used primers A109F/A1000R and the second introduced a 5' GC clamp using A771F-GC/A975R (Supplementary Table 6). The same method was used to screen for a shift in the archaeal community across root compartments. One round of PCR was used for bacterial DGGE using the primers PRK341F-GC/518R to introduce a 5' GC clamp, or for archaeal *amoA* DGGE using CrenamoA23f/A616r (Supplementary Table 6). PCR conditions are indicated in Supplementary Table 7. An 8% polyacrylamide gel was made with a denaturing gradient of 40–80% (2.8 M urea / 16% (vol/vol) formamide, to 5.6 M urea / 32% (vol/vol) formamide), and a 6% acrylamide stacking gel with 0% denaturant. 2–8 µl of PCR product was loaded per well for each sample and the gel was loaded into an electrophoresis tank filled with 1x Tris acetate EDTA (TAE) buffer (242 g Tris base, 57.1 ml acetic acid, 100 ml 0.5 M EDTA pH 8.0). Electrophoresis ran at 0.2 amps, 75 V and 60 °C for

16 h. After washing, gels were stained in the dark using 4 µl of SYBR gold nucleic acid gel stain (Invitrogen™) in 400 ml 1x TAE buffer. After 1 h, gels were washed twice before imaging using a Bio-Rad Gel Doc XR imager. DGGE gels from SIP fractions (Supplementary Figures 2 and 5) were used to identify heavy and light fractions to be pooled and used for sequencing, see Supplementary Table 4.

#### DNA sequencing and analysis

All 16S rRNA genes were amplified using primers specific to the archaeal (A109F/A1000R) or bacterial (PRK341F/MPRK806R) gene (Supplementary Table 6). The fungal 18S ITS2 region was amplified using primers specifically targeting fungi (fITS7Fw/ITS4Rev\_2) to avoid *Triticum aestivum* ITS2 amplification (Supplementary Table 6). No fungal ITS2 amplicon could be obtained from the endosphere of Levington F2 compost-grown plants. PCR conditions are indicated in Supplementary Table 7. Purified PCR products were sent for paired-end sequencing using an Illumina MiSeq platform at Mr. DNA (Molecular Research LP, Shallowater, Texas, USA). The bacterial 16S rRNA gene was sequenced using the PRK341F/MPRK806R primers (465 bp). The archaeal 16S rRNA gene was sequenced using the A0349F/A0519R primers (170 bp). The fungal ITS2 region was sequenced with the fITS7Fw/ITS4Rev\_2 primers (350 bp). See Supplementary Table 6 for primer sequences. Upon receipt, all sequencing reads were further processed using the software package quantitative insights into microbial ecology 2 (Qiime2 [48]) version 2019.7. Paired-end sequencing reads were demultiplexed and then quality filtered and denoised using the DADA2 plugin version 1.14 [49]. Reads were trimmed to remove the first 17–20 base pairs (primer dependent, see Supplementary Table 8) and truncated to 150–230 base pairs to remove low quality base calls (dependent on read quality and amplicon length, see Supplementary Table 8). Chimeras were removed using the consensus method and default settings were used for all other analyses. For taxonomic assignments Bayesian bacterial and archaeal 16S sequence classifiers were trained against the SILVA [50] database version 128 using a 97% similarity cut off. For the fungal ITS2 reads, the Bayesian sequence classifier was trained against the UNITE [51] database version 8.0 using a 97% similarity cut-off. Taxonomy-based filtering was performed to remove contaminating mitochondrial, chloroplast and *Triticum* sequences (Supplementary Table 9), remaining sequences were used for all further analyses. Taxonomy-based filtering was not required for the fungal dataset. For all datasets, taxonomic identification was validated via the National Centre for Biotechnology Information (NCBI) basic local alignment search tool (BLAST) [52],

which verified correct taxonomic identification for the top three most abundant OTUs.

Statistical analysis was performed using *R* version 3.6.2 [53]. The package *vegan* version 2.5–7 [54] was used to calculate Bray Curtis dissimilarities and conduct similarity percentages breakdown analysis (SIMPER [55]). Permutational Multivariate Analysis of Variance (Permanova) analyses were conducted using Bray Curtis dissimilarity matrices and the *adonis* function in *vegan*. Bray Curtis dissimilarities were also used for principle co-ordinate analysis (PCoA) which was performed using the packages *phyloseq* version 1.3 [56] and *plyr*. Differential abundance analysis was performed using DESeq2 in the package *microbiomeSeq* version 0.1 [57]. Given the low number of reads which remained in some samples after taxonomy-based filtering (Supplementary Table 9), a base mean cut off of 200 for the field and pot metabarcoding experiments, or of 400 for the stable isotope probing experiment, was applied to the DESeq2 output to eliminate possible false positives resulting from low sequencing depth. If a taxon had a base mean > 200 and a significant *p*-value in one or more comparison, data for that taxon was plotted in Fig. 3 for all comparisons. For details see Supplementary Tables 4, 10, 11, 12, 13, 14, 15 and 16.

#### Real-time quantitative PCR

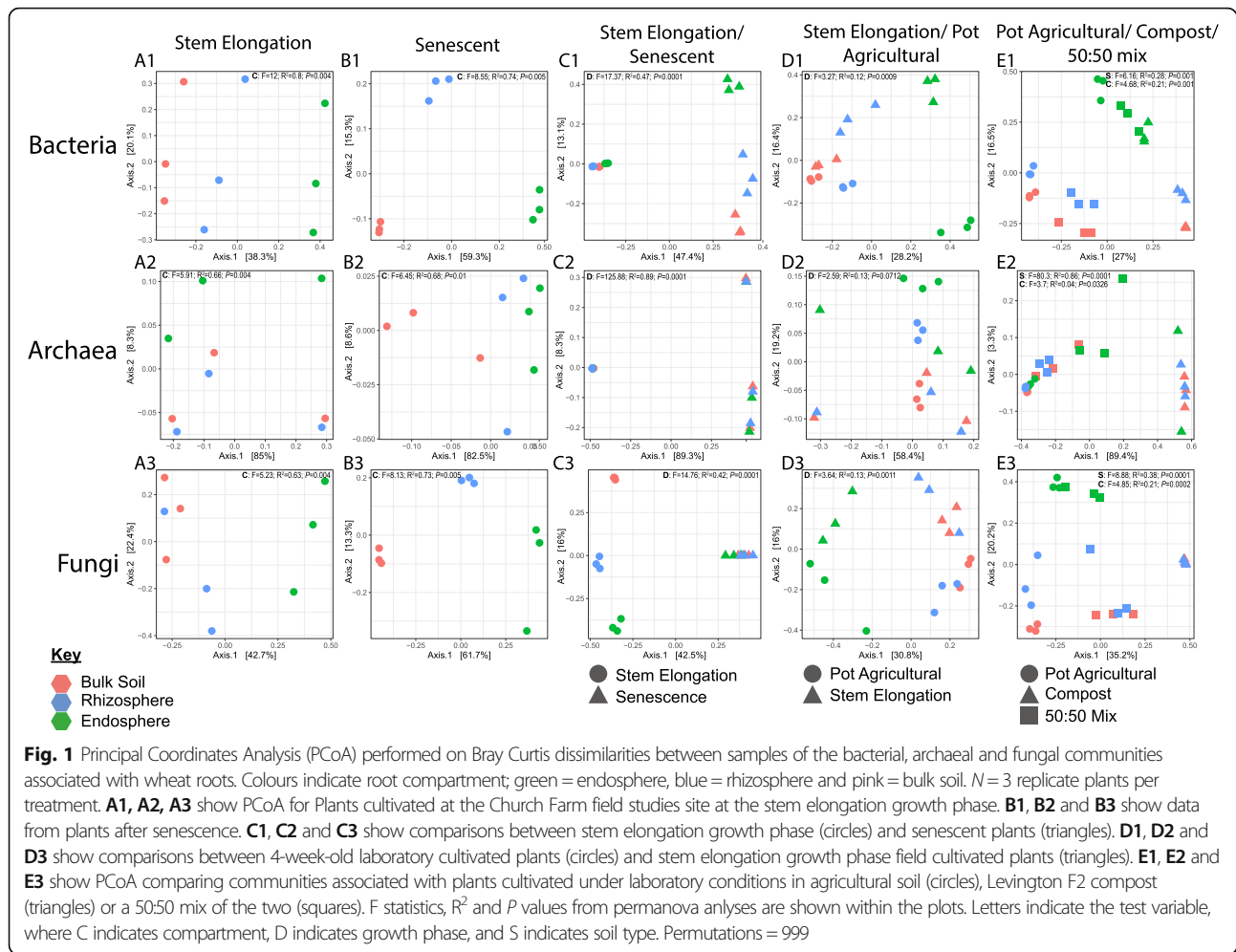
The abundance of bacterial or archaeal 16S rRNA genes and of fungal 18S rRNA genes was determined by qPCR amplification of these genes from DNA extracts. Bacterial 16S rRNA abundance was quantified using bacteria-specific primers Com1F/769r, as previously described [58]. Archaeal 16S rRNA gene abundance was quantified using the archaeal specific A771f/A957r primers, as previously described [59]. Fungi-specific primers, as previously described [60], FR1F/FF390R were used to quantify 18S rRNA gene abundance and examine <sup>13</sup>C labelling of the fungal community for the SIP fractions. Primer sequences are presented in Supplementary Table 6. The qPCR was performed using the Applied Biosystems QuantStudio 1 Real-Time PCR System (Applied Biosystems, Warrington, UK) with the New England Biolabs SYBR Green Luna® Universal qPCR Master Mix (New England Biolabs, Hitchin, UK). PCR mixtures and cycling conditions are described in Supplementary Table 7. Bacterial, fungal and archaeal qPCR standards were generated using a set of primers enabling amplification of the full length bacterial or archaeal 16S rRNA gene or fungal 18S rRNA gene, cloned into the Promega pGEM®-T Easy Vector system, and the correct sequence was validated by Sanger sequencing (Supplementary Table 6). After purification, the standard was diluted from  $2 \times 10^7$  to  $2 \times 10^0$  copies /  $\mu$ l in duplicate and ran alongside all qPCR assays. Ct values from standard dilutions were plotted as a standard curve and used to

calculate 16S/18S rRNA gene copies / 50 ng DNA extract. Amplification efficiencies ranged from 90.9 to 107% with  $R^2 > 0.98$  for all standard curve regressions. All test samples were normalised to 50 ng of template DNA per reaction and ran in biological triplicate. PCR products were all analysed by both melt curves and agarose gel electrophoresis which confirmed amplification of only one product of the expected size. For statistical comparison of the average 16S rRNA or 18S rRNA gene copy number between samples ANOVA and linear models, followed by Tukey post-hoc was run in *R* [53].

## Results

### The microbial community associated with *Triticum aestivum* var. Paragon

To gain initial insights into the microbial communities associated with wheat roots, we characterised the microbial community associated with field-grown wheat sampled during the stem elongation growth phase. The diversity of microbes in the bulk soil, rhizosphere, and endosphere compartments was investigated using 16S rRNA gene (for bacteria and archaea) and ITS2 (for fungi) metabarcoding, respectively. The bacterial and fungal communities differed significantly across compartments (bacterial Permanova:  $R^2 = 0.8$ ,  $p < 0.01$ ; fungal Permanova:  $R^2 = 0.63$ ,  $p < 0.01$ ). This was particularly the case for the rhizosphere and endosphere compartments compared to bulk soil, as demonstrated by principal coordinates analysis (PCoA) (Fig. 1; A1, A3). Community profiles did not indicate a strong shift in the archaeal community across compartments at the family level (Fig. 2; C1), but statistical analysis indicated a significant effect of compartment on archaeal community composition at the OTU level (archaeal Permanova:  $R^2 = 0.66$ ,  $p < 0.01$ ), with PCoA indicating that differences in the endosphere may mostly be responsible for this shift (Fig. 1; A2). For the bacterial community, the family *Streptomyetaceae* showed the greatest average relative abundance in the endosphere (25.12%), followed by *Burkholderiaceae* (11.99%) and *Sphingobacteriaceae* (7.75%). In the rhizosphere the relative abundance of *Streptomyetaceae* was much lower (2.58%), while *Micrococcaceae* were most abundant (8.43%), followed by *Burkholderiaceae* (7.41%) and *Sphingobacteriaceae* (6.58%) (Fig. 2; A1). The fungal endosphere community was dominated by the Xyariales order (32.9%), followed by the class Sordariomycetes (14.33%), then the *Metarhizium* (10.44%). For the rhizosphere, however *Metarhizium* had the greatest relative abundance (27.36%), followed by the Chaetothyriales order (12.32%) and the Sordariomycetes (9.23%). The archaeal community was overwhelmingly dominated by the AOA family *Nitroso-sphaeraceae* (endosphere 89.77%, rhizosphere 81.55%). Differential abundance analysis demonstrated that the

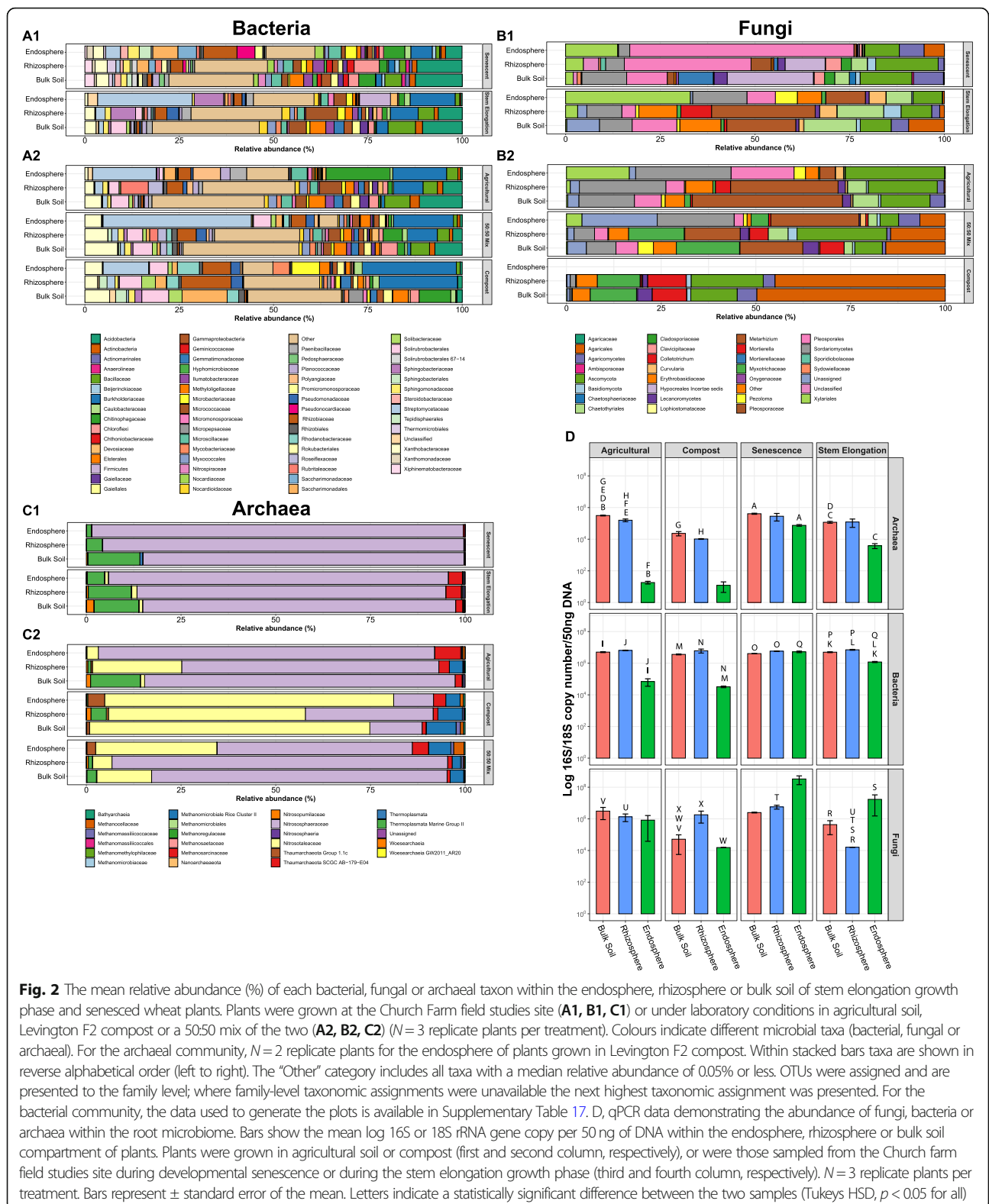


abundance of 14 bacterial families, including *Streptomyces*, *Burkholderiaceae* and *Sphingobacteriaceae*, increased significantly within the rhizosphere and/or the endosphere relative to the bulk soil (Fig. 2; A1, Fig. 3; A1). The families *Streptomyces* (16.4% contribution,  $p < 0.01$ ) and *Burkholderiaceae* (6.1% contribution,  $p < 0.01$ ) were the two most significant contributors to the bacterial community shift as confirmed by SIMPER analysis (Supplementary Table 1). For the fungal community, most significantly differentially abundant groups were reduced in abundance compared to in the bulk soil, however one taxon was significantly more abundant in the rhizosphere (*Mortierellaceae*), and one was significantly more abundant in the endosphere (*Parmeliaceae*) (Fig. 3; A2). No significantly differentially abundant archaeal families were found.

Quantitative PCR (qPCR) was used to estimate the total abundance of archaeal and bacterial 16S rRNA genes and fungal 18S rRNA genes (Fig. 2; D). This showed that bacterial 16S rRNA gene copy number was significantly greater within the bulk soil ( $4.98 \times 10^6$  16S rRNA gene copies / 50 ng DNA) and the rhizosphere

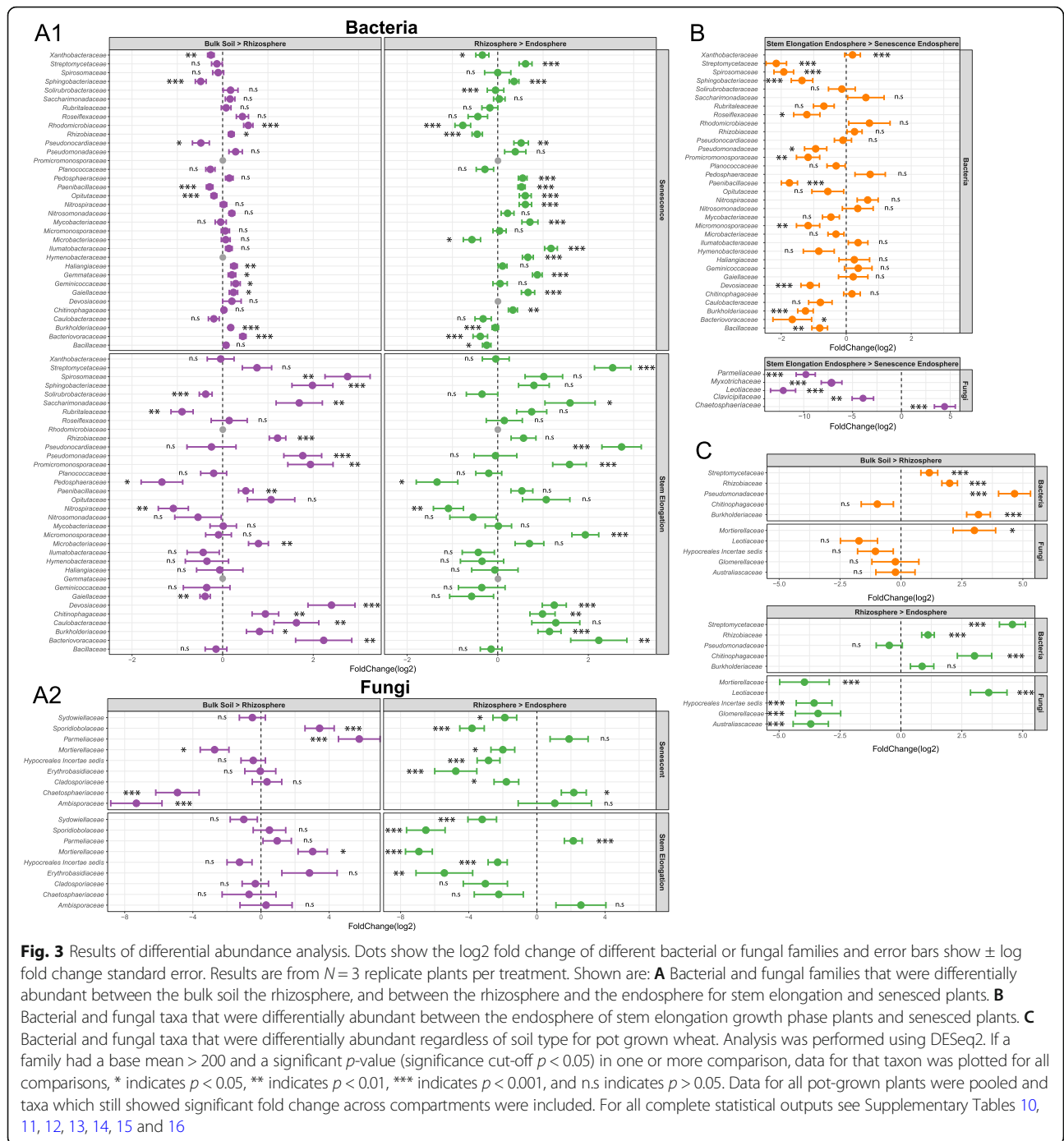
( $7.03 \times 10^6$  16S rRNA gene copies / 50 ng DNA) compartments when compared to the endosphere ( $1.19 \times 10^6$  16S rRNA gene copies / 50 ng DNA) (Tukey's HSD,  $p < 0.01$  for both comparisons). Fungi outnumbered bacteria and archaea by more than an order of magnitude within the endosphere ( $1.72 \times 10^7$  18S rRNA gene copies / 50 ng DNA) (Fig. 2; D). This may indicate that fungi are more abundant within the endosphere but could also be a product of the higher 18S rRNA gene copy number per genome within some fungi [61]. When comparing bulk soil to the endosphere, archaeal 16S rRNA gene copy number decreased by two orders of magnitude in the endosphere ( $1.18 \times 10^6$  16S rRNA gene copies / 50 ng bulk soil DNA,  $3.89 \times 10^3$  16S rRNA gene copies / 50 ng endosphere DNA), while the fungal 18S rRNA gene copy number increased by two orders of magnitude ( $4.32 \times 10^5$  18S rRNA gene copies / 50 ng bulk soil DNA,  $1.72 \times 10^7$  18S rRNA gene copies / 50 ng endosphere DNA). Despite this, root compartments were not found to significantly influence the abundance of archaea or fungi (ANOVA,  $p > 0.05$ ). This is likely due to high variation across the replicates and could indicate





more stochastic root colonisation by fungi and archaea. Compared to bacteria or fungi there were at least three orders of magnitude fewer archaeal 16S rRNA gene

copies detected within the endosphere. Despite the lower 16S rRNA gene copy number found in most archaeal genomes [62] this likely demonstrates archaea colonise the



root in much lower numbers than the other root microbiota.

**The effect of developmental senescence on the root community**

We next aimed to investigate the effect of developmental senescence on the root microbial community and, specifically, to identify microbial taxa associated with the roots of living plants that decline in number during

senescence. Developmental senescence is the final stage in wheat development and the point at which nutrients become remobilised from the plant into the developing grain. At this point the plants are no longer green or actively growing. Senescent plants were sampled from the same site as the plants sampled during stem elongation growth phase. Analysis of rRNA gene copy number (from qPCR experiments) showed that plant growth phase significantly influenced the abundance of bacteria

(growth phase in a linear model:  $F$ -value = 4.86,  $p < 0.05$ ) and archaea ( $F$ -value = 10.55,  $p < 0.01$  in a linear model) within the root microbiome (Fig. 2; D). Comparing specific compartments for each group showed that, while there was no significant difference in the abundance of bacteria within the bulk soil or rhizosphere sampled at either growth phase (Tukey's HSD,  $p > 0.05$ ), the abundance of bacteria increased significantly within the endosphere after senescence (Tukey's HSD,  $p < 0.001$ ). Fungal 18S rRNA gene copy number was significantly reduced in the rhizosphere after senescence (Tukey's HSD,  $p < 0.05$ ) but increased by an order of magnitude in the endosphere, although this increase was not statistically significant (Tukey's HSD,  $p > 0.05$ ), likely due to variation across replicates. For archaea there were no statistically significant differences in 16S rRNA gene copy number between the two growth phases for any compartment. Both fungal and bacterial community composition differed significantly across the three different root compartments of senescent plants, as clearly demonstrated by PCoA (Fig. 1; B1, B2, B3) and Permanova analysis for all three microbial groups (Supplementary Table 2). In addition to this, PCoA showed a clear difference between the microbial communities associated with senescent or stem elongation growth phase plants, however, they also indicated that the root community was much more variable for senescent plants compared to those in the stem elongation phase (Fig. 1; C1, C2, C3). Permanova analysis corroborates this observation as, whilst this showed a significant effect of plant growth phase on overall community composition for all three microbial groups (Permanova, bacterial:  $R^2 = 0.47$ ,  $p < 0.001$ , archaeal:  $R^2 = 0.89$ ,  $p < 0.001$ , fungal:  $R^2 = 0.42$ ,  $p < 0.001$ ), betadisper analysis indicated that microbial community dispersion was not equal between the two growth phases ( $p < 0.01$  for all), i.e. the senescent growth phase showed greater community variability compared to the stem elongation phase.

For individual taxa, differential abundance analysis showed that sixteen bacterial and fungal taxa were significantly less abundant within the endosphere of senescent plants than at the stem elongation growth phase ( $p < 0.05$ , Supplementary Table 14). The largest change in abundance was a two-fold reduction in the family *Streptomycetaceae* and there was also a significant reduction in the relative abundance of the families *Burkholderiaceae* and *Sphingobacteriaceae* in senescent plants (Fig. 3; A1, B). This implies that these taxa may require input from the living plant in order to persist within the endosphere. No archaeal taxa demonstrated significant changes in abundance across root compartments between growth phases. The archaeal community was consistently dominated by the AOA family *Nitroso-sphaeraceae*. For the fungal community, differential

abundance analysis indicated that the abundance of most taxa was significantly reduced in senescent plants, with the exception of *Chaetosphaeriaceae* which showed a four-fold increase during senescence when compared to the stem elongation phase.

#### Laboratory-grown *Triticum aestivum* var. Paragon plants provide an agriculturally relevant model

Root associated microbial communities can be influenced by a multitude of abiotic factors, including crop cultivation practices and climatic conditions [63]. To test whether the microbiomes of laboratory-grown plants are comparable to those grown in the field, plants were grown for 4 weeks under laboratory conditions in soil collected from the Church Farm site and the composition of the root microbiome was profiled using 16S rRNA gene and ITS2 metabarcoding. Laboratory-grown plants were sampled during root growth phase, whereas field plants were sampled during the late stem elongation growth phase, meaning laboratory-grown plants were sampled much earlier in the life cycle. However, the same major microbial families were present within the endosphere of both groups of plants (Fig. 2; A, B, C). PCoA plots indicated a shift in the endosphere community when comparing field to pot grown wheat (Fig. 1; D1, D2, D3). However, whilst statistical analysis did indicate a significant difference between the overall bacterial and fungal communities associated with the two groups of plants (Permanova, bacterial:  $R^2 = 0.12$ ,  $p < 0.001$ , fungal:  $R^2 = 0.13$ ,  $p < 0.01$ , archaeal:  $R^2 = 0.13$ ,  $p > 0.05$ ), subsequent pairwise analysis found no significant difference between any specific compartments (Supplementary Table 2). qPCR indicated that the overall abundance of bacteria and archaea was significantly different between the two groups of plants ( $p < 0.05$  in linear models for both microbial groups). While there were significantly more archaea within the bulk soil associated with pot-grown plants (Tukey's HSD,  $p < 0.01$ ) post-hoc analysis did not show a significant difference in the abundance of either archaea or bacteria in the root associated compartments between the different groups of plants (Tukey's HSD,  $p > 0.05$  for all). A significantly greater quantity of fungi was detected within the rhizosphere of laboratory-grown plants (Tukey's HSD,  $p < 0.05$ ) and we also observed lower quantities of all groups within the endosphere (Fig. 2; D). Overall, this analysis shows that there is likely a lower microbial abundance within the endosphere of laboratory-grown root growth phase plants, but that any effects on community composition were subtle and mostly restricted to low abundance taxa. As bacterial, fungal, and archaeal communities contained the same major taxa within the endosphere, we conclude that laboratory-grown plants could serve as an approximate experimental analogue for agriculturally cultivated

wheat plants when studying the composition of the root microbial community.

#### Does *Triticum aestivum* var. Paragon select for specific microbial taxa?

Microbial communities and their functions can differ dramatically between different soils and, as a consequence, soil parameters play a central role in shaping the microbial communities associated with plants [20, 64]. To determine if the enrichment of specific microbial taxa and, in particular, the dominance of *Streptomycetaceae* and *Burkholderiaceae*, within the wheat root endosphere was driven by the soil community or by the host, *T. aestivum* var. Paragon was grown in two contrasting soil types (agricultural soil or compost), and a 50:50 mixture of the two. It was reasoned that if *Streptomycetaceae* and *Burkholderiaceae* were dominant only in the agricultural soil and the mixed soil, then certain strains within the agricultural soil might be particularly effective at colonising the endosphere. However, if *Streptomycetaceae* and *Burkholderiaceae* were dominant in the endosphere across all three soil conditions, this would indicate that when present, this family is selectively recruited to the wheat root microbiome. The microbiome was compared between four-week-old (root growth phase) plants grown in Church Farm agricultural soil, Levington F2 compost, and a 50:50 (vol/vol) mix of the two soils under laboratory conditions. Church Farm soil and Levington F2 compost are starkly contrasting soil environment, see Supplementary Table 3 for soil parameters.

It is well documented that the soil microbial community is a major determinant of endosphere community composition, as endophytic microbes are acquired by plants from the soil [6]. The present study corroborates this observation as PCoA showed clear clustering of communities by soil type, indicating that soil type was an important determinant of the root-associated community composition (Fig. 1; E1, E2, E3). For the bacterial and archaeal communities, Permanova corroborated a significant effect of soil type on bacterial community composition for all compartments (Supplementary Table 2). For the fungal community, Permanova also showed significant effect of soil type on the bulk soil and rhizosphere communities (Supplementary Table 2). For plants cultivated in Levington F2 compost, no data on the fungal community composition within the endosphere could be retrieved. Thus, no statistical comparison could be made. The bacterial communities were distinct between the bulk soil, rhizosphere, and endosphere. This indicated that, while the soil had a significant impact on the composition of the root associated communities, the plant also selects for specific microbial taxa in all the tested soils (Fig. 1; E1). PCoA showed a detectable

rhizosphere effect (Fig. 1; E1) but, consistent with previous studies [24, 30], we observed a rhizosphere effect for *T. aestivum* var. Paragon that was subtle as there were only minor differences between the community composition of bulk soil and rhizosphere communities (Fig. 2; A, B, C). A SIMPER test revealed that, regardless of soil type, *Streptomycetaceae* (14.6% contribution,  $p < 0.01$ ) and *Burkholderiaceae* (10.1% contribution,  $p < 0.01$ ) were the main taxa driving the community shift from bulk soil to endosphere (Supplementary Table 1). This is supported by the fact that *Streptomycetaceae* and *Burkholderiaceae* were major components of the endosphere bacterial communities under all conditions (Fig. 2). Differential abundance analysis demonstrated a significant increase in the abundance of bacterial families *Burkholderiaceae*, *Chitinophagaceae*, *Pseudomonadaceae*, *Rhizobiaceae* and *Streptomycetaceae* within the rhizosphere and/or endosphere across all soil types (Fig. 3; C). Enrichment of these groups was correlated with the reduced abundance of some fungal taxa loosely associated with pathogenicity within the endosphere and rhizosphere (*Australiascaceae* [65], *Glomerellaceae* [66, 67] and *Hypocreale* [68]), and an increased abundance of one taxon loosely associated with beneficial mycorrhiza (*Leotiaceae* [69–71]) (Fig. 3; C).

Further to this, qPCR experiments were performed to compare the abundance of archaea, bacteria, and fungi within the roots of plants cultivated in the agricultural soil or Levington F2 compost. No significant effect of soil type was observed for either fungi or bacteria (ANOVA,  $p > 0.05$  for both) (Fig. 2; D). However, soil type had a significant effect on the abundance of archaea ( $p < 0.001$ ); there were significantly greater numbers of archaea within the agricultural bulk soil and rhizosphere compartments when compared to those for Levington F2 compost (Tukey's HSD,  $p < 0.001$  for both), but there was no significant difference in the archaeal load detected within the endosphere (Tukey's HSD,  $p > 0.05$ ). The lower abundance of archaea within Levington F2 compost is surprising given the higher nutrient levels in this soil, and particularly the higher levels of ammonium (Supplementary Table 3).

The archaeal community was dominated by two families of AOA (*Nitrososphaeraceae* and *Nitrosotaleaceae*), which were abundant in all root compartments. *Nitrosotaleaceae* dominated in the more acidic Levington F2 compost whereas *Nitrososphaeraceae* was most abundant in the neutral pH Church Farm soil (Fig. 2; C). While soil type was a major determinant of community composition, no selection of specific archaeal lineages within the endosphere was detected by SIMPER or differential abundance analysis, and PCoA did not show a strong effect of compartment on community composition (Fig. 1; E2). Contrary to this, there was a small but significant shift in the archaeal community composition

overall across compartments (archaeal Permanova:  $R^2 = 0.86$ ,  $p = 0.001$ ), and a betadisper analysis was not significant ( $p > 0.01$ ), demonstrating this was not due to difference in dispersion between compartments (Fig. 2; C2). Together, these findings might suggest that there is no major selection of archaeal taxa by the wheat roots. However, denaturing gradient gel electrophoresis (DGGE) analysis performed on the archaeal 16S rRNA and *amoA* genes showed a clear shift in the archaeal community across compartments (Supplementary Figure 1). Unfortunately the archaeal 16S rRNA gene database lacks the established framework of its bacterial counterpart [72] and this, coupled with the lack of known diversity or strain characterisation within many archaeal taxa, makes it difficult to achieve good taxonomic resolution from short read amplicon sequencing of the archaeal 16S rRNA gene. We hypothesised therefore that this discrepancy between DGGE and amplicon sequencing arose from the lack of detailed taxonomic representation within the database used to analyse the sequencing data. Despite these limitations, this study has revealed that AOA dominate the archaeal community associated with wheat roots regardless of soil type, and that the abundance of archaea within the root is highest in agricultural soil and increases later in the life cycle of the plant.

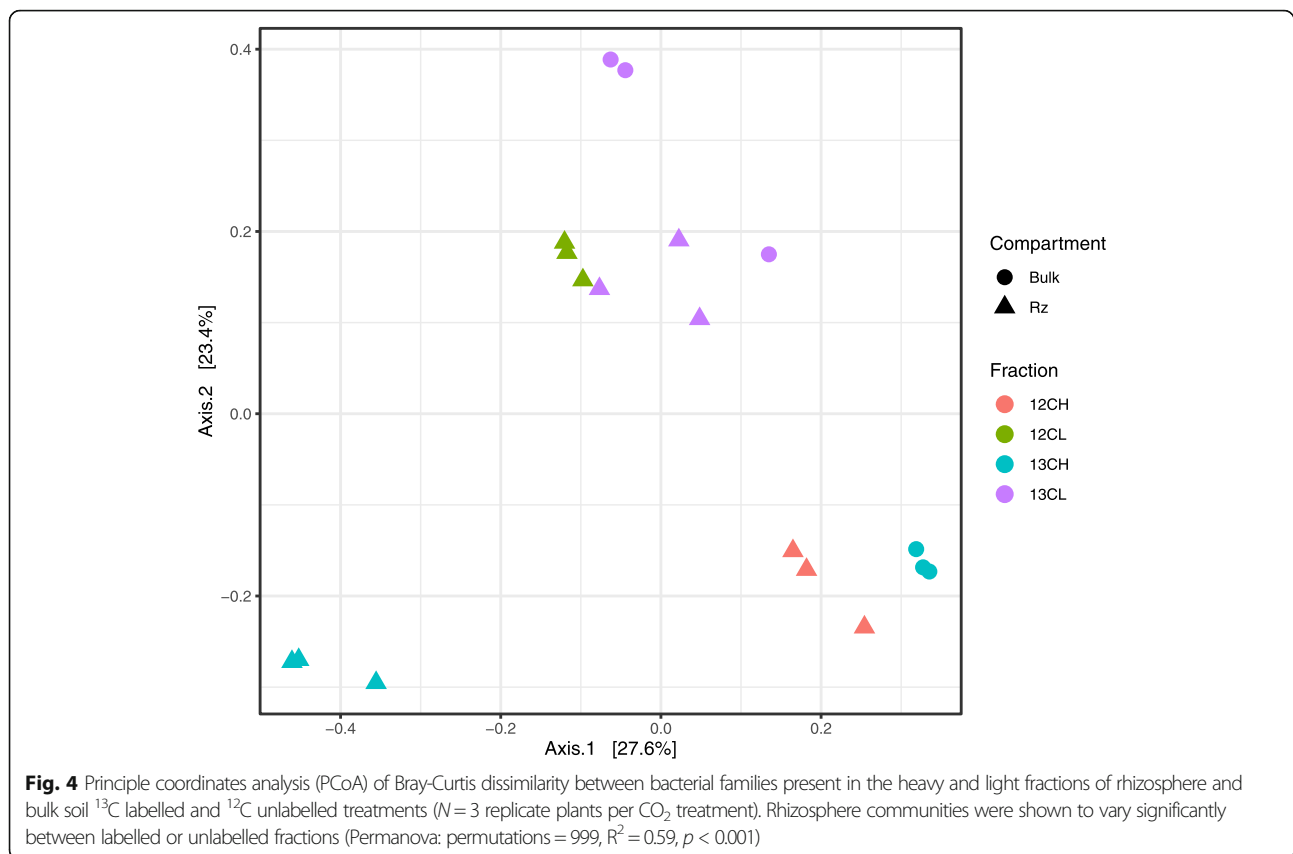
#### Identification of root exudate utilising microbes using $^{13}\text{C}$ CO<sub>2</sub> DNA stable isotope probing

Plants exude 30–40% of the carbon they fix from the atmosphere as root exudates [9]. These compounds can be utilised as a carbon source by microbes residing within and in the vicinity of the root and root exudates could be tailored by the plant to select particular microbial species from the soil. Thus, we aimed to identify the microbial taxa that wheat can support via  $^{13}\text{C}$ CO<sub>2</sub> DNA-SIP. Briefly, wheat was incubated in  $^{13}\text{C}$ CO<sub>2</sub> for 2 weeks. During this period, the “heavy”  $^{13}\text{C}$ CO<sub>2</sub> becomes photosynthetically fixed into carbon-based metabolites and some of these  $^{13}\text{C}$  labelled compounds are exuded from the roots. Microbial utilisation of these compounds will, in turn, result in the  $^{13}\text{C}$  label being incorporated into the DNA backbone of actively growing microorganisms. Heavy and light DNA can be separated via density gradient ultracentrifugation and the fractions are then analysed using amplicon sequencing to identify metabolically active microbes. The two-week labelling period was chosen to minimise the probability of labelling via cross feeding by secondary metabolisers [39, 47]. Labelling of the bacterial community in the rhizosphere and endosphere was confirmed using DGGE (Supplementary Figures 2 and 5), then heavy and light fractions were pooled and analysed by 16S rRNA gene sequencing (as defined in Supplementary Table 4). The same DGGE experiment was performed using primers targeting archaea and did not indicate labelling and therefore no

sequencing of archaea was carried out (Supplementary Figure 3). For fungi, PCR amplification of the ITS2 region for DGGE did not consistently yield products for all fractions, thus DGGE could not be performed. Instead, qPCR was used and did not detect labelling of the fungal community (Supplementary Figure 4) so no sequencing was performed for the fungal community.

PCoA indicated that bacterial communities within endosphere samples were highly variable (Supplementary Figure 5) and there was no significant difference between  $^{13}\text{C}$ -labelled heavy and light fractions (Permanova:  $R^2 = 0.29$ ,  $p > 0.1$ ). This means the endosphere dataset was too variable to draw any conclusions from the current study about the utilisation of host derived carbon within the endosphere (Supplementary Figure 5). For the rhizosphere however, the replicates were consistent, and PCoA revealed that the bacterial community in the  $^{13}\text{C}$  heavy fraction was distinct from that of the  $^{12}\text{C}$  heavy DNA (control) fraction and distinct from the  $^{13}\text{C}$  DNA and  $^{12}\text{C}$  light DNA fractions (Fig. 4). In addition, the community was significantly different in the  $^{13}\text{C}$  heavy DNA fraction compared to the unlabelled samples, suggesting that a distinct subset of bacteria was incorporating root-derived carbon (Permanova:  $R^2 = 0.59$ ,  $p < 0.001$ ). To control for CO<sub>2</sub> fixation by soil autotrophs the  $^{13}\text{C}$  heavy fraction was compared to a  $^{13}\text{C}$  unplanted soil control using PCoA; this analysis indicated that the  $^{13}\text{C}$  heavy DNA fraction was distinct from the  $^{13}\text{C}$  bulk soil control (Fig. 4). After these comparisons, we could be confident that the shift in community composition within the  $^{13}\text{C}$  heavy DNA fraction was driven by microbes within the rhizosphere actively utilising root exudates. Differential abundance analysis was performed to identify the taxa driving these shifts. Exudate metabolisers were defined as taxa showing significantly greater abundance within  $^{13}\text{C}$  heavy DNA fractions when compared with both the  $^{13}\text{C}$  light fractions and the  $^{12}\text{C}$  control heavy fractions. Above the abundance threshold, we identified 9 exudate-utilising bacterial taxa (Fig. 5, Supplementary Table 5). While *Streptomycetaceae* were not among these, three other core enriched bacteria were found to utilise root exudates, *Pseudomonadaceae*, and both *Comamonadaceae* and *Oxalobacteriaceae*, which likely belonged to the *Burkholderiaceae*. As defined by the Genome Taxonomy Database [73], *Comamonadaceae* and *Oxalobacteriaceae* are now classified as genera *Comamonas* and *Oxalobacter* within the *Burkholderiaceae* family.

Six other taxa were also found to utilise root exudates, *Verrucomicrobiaceae*, *Enterobacteriaceae*, *Micrococcaceae*, *Paenibacillaceae*, *Cytophagaceae* and *Fibrobacteraceae*. The most abundant of these taxa were the *Enterobacteriaceae*, although this group was not identified within any other dataset within this study. However, the class to

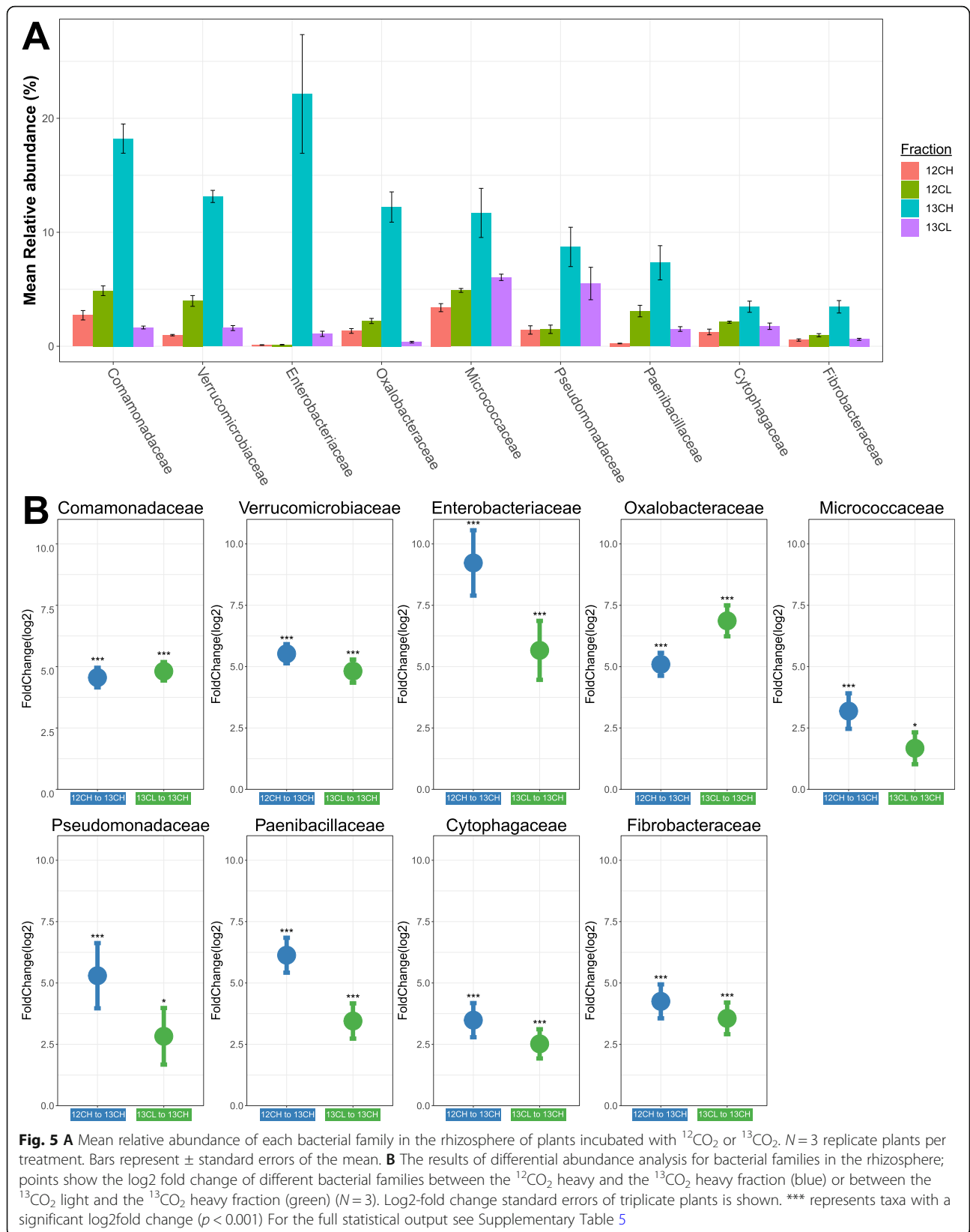


which these families belong, the Gammaproteobacteria, was identified in all root samples, but was excluded from differential abundance analysis due to its high-level taxonomic identification. To explore whether these Gammaproteobacteria OTUs could indeed belong to the Enterobacteriaceae family, the reads were extracted and manually ran through NCBI BLAST [52]; this however did not yield any alignments with an identity  $> 95\%$ , and thus revealed no additional information about the identity of the Gammaproteobacteria reads.

While not identified as a core enriched taxa, *Micrococcaceae* were detected at low quantities within the roots of all plants cultivated within agricultural soil. Whilst this family constituted a small percentage of the microbial community within Levington F2 compost, *Micrococcaceae* were not detected within the endosphere of plants cultivated in Levington F2 compost, indicating that they were only able to colonise the root from agricultural soil (Fig. 2, Supplementary Table 17). *Fibrobacteraceae*, *Cytophagaceae*, and *Paenibacillaceae* were all identified by differential abundance analysis as candidate core enriched endosphere or rhizosphere taxa, as all showed a significant increase in their abundance within the root associated compartments regardless of soil type (Supplementary Table 12). They were abandoned as candidate core enriched taxa, however, as

their abundance fell below the threshold that was selected to exclude false positives resulting from low abundance taxa. Their identification as exudate utilisers provides limited evidence that these three taxa may indeed be core enriched members of the root community. Indeed, *Paenibacillaceae* were enriched within the rhizosphere at the stem elongation growth phase (Fig. 3 A). The abundance of this group within the endosphere was significantly lower after senescence, and the same pattern was observed for core enriched exudate utilisers *Pseudomonadaceae* and *Burkholderiaceae* (Fig. 3 B). Together this indicates that taxa reliant on root exudates may be unable to persist within the root after developmental senescence.

Within the  $^{13}\text{C}$  unplanted soil control, differential abundance analysis indicated that six taxa were significantly enriched in the heavy DNA fraction compared to the light fraction these taxa are hypothesised to fix  $^{13}\text{CO}_2$  autotrophically (Supplementary Table 10). Only one taxon was  $^{13}\text{C}$ -labelled in both the rhizosphere and unplanted soil, *Intrasporangiaceae*, and thus was excluded from the list of root exudate utilising bacterial taxa. While microbes belonging to this family are capable of photosynthesis, they also have genomes with high GC content, and as such they may be overrepresented in heavy fractions.



## Discussion

In this work we profiled the microbial communities in the rhizosphere and endosphere of the UK elite Spring bread wheat *T. aestivum* variety Paragon. We identified the core microbial families associated with the rhizosphere and endosphere of these plants and the subset of microorganisms assimilating plant-derived carbon in the rhizosphere. This study revealed that plant developmental senescence induces shift in the root-associated microbial communities and an increase in microbial abundance in the plant endosphere. Concurrent with established literature [6, 21, 74] we found the soil inoculum to be a major driver of root community composition. Given the contrasting range of soils, wheat varieties, developmental timepoints, and growth management strategies used across studies, drawing direct comparisons is often challenging. For example Schlatter et al. identified *Oxolabacteraceae*, *Comamonadaceae* and *Chitinophaga* as core rhizobacteria for the wheat cultivar *Triticum aestivum* L. cv. Louise [29]. Our work corroborates this observation for *T. aestivum* var. Paragon, all these taxa were identified by SIP as exudate utilising microbes. However, many of the core taxa identified by Schlatter et al. were not identified by the present work. Similarly, for the endosphere community, Kuźniar and colleagues identified *Flavobacterium*, *Janthinobacterium*, and *Pseudomonas* as core microbiota for both cultivars tested, and *Paenibacillus* as a core taxon for *T. aestivum* L. cv. Hondia [28]. We identified *Pseudomonadaceae* as a core component of the *T. aestivum* var. Paragon endosphere microbiome and, while *Paenibacillaceae* were not enriched in the endosphere consistently, we did identify this family as an exudate utiliser within the rhizosphere. *Streptomycetaceae* were not identified by the study of Kuźniar and colleagues. While these combined results consistently imply a role for common taxa such as *Pseudomonadaceae* or members of the *Burkholderiaceae* family, it cannot explain the differences observed in colonisation by other taxa, and in particular *Streptomycetaceae*. While it is likely this is largely driven by soil type, there is some evidence that for wheat, similarly to barley [11], plant genotype may be responsible for these differences [24, 28, 32, 44]. In a study which used the same Church Farm field site as our work, *T. aestivum* var. Paragon was previously reported to be an outlier compared to other wheat varieties, with a particularly distinct rhizosphere and endosphere community [24]. Further studies are needed to fully assess how wheat rhizosphere and endosphere communities vary across different wheat cultivars and soil environments, and which of these factors has the greatest influence.

While only slight differences were observed between root-growth phase laboratory cultivated plants and stem

elongation phase field cultivated plants, significant changes in the abundance of numerous bacterial and fungal taxa occurred at the onset of plant developmental senescence. To our knowledge, the wheat root community has not previously been assessed after senescence, though development has been shown to significantly alter the wheat rhizosphere community [22, 23]. One fungal group, *Chaetosphaeriaceae*, was significantly enriched as the plant senesced. This family represents a relatively diverse group of fungi, although members of this group such as *Chaetosphaeria* are known to reproduce within decomposing plant tissues, which may explain the four-fold increase in abundance after senescence [75]. In terms of the overall fungal community composition (Fig. 2; B1), the greatest change during senescence was in the Pleosporales group, and this may also contribute to the observed increase in fungal abundance during senescence. This group was excluded from the differential abundance analysis which focused on lower taxonomic ranks. Pleosporales is an order of fungi containing over 28 families [76], and such a high diversity makes the ecological role of this group difficult to postulate. Some families within the Pleosporales are associated with endophytic plant parasites [76], including necrotrophic pathogens of wheat *Pyrenophora tritici-repentis* and *Parastagonospora nodorum* [77]. Necrotrophic pathogens specialise in colonising and degrading dead plant cells, and senescent tissues are thought to provide a favourable environment for necrotrophs [37]. It is interesting to note that this increased fungal colonisation correlated with reduced abundance of fungi-suppressive endophytic bacteria such as *Streptomycetaceae* [78, 79] and *Burkholderiaceae* [80] during developmental senescence. The present work, however, cannot provide any direct evidence of a causative relationship driving this correlation.

AOA were found to dominate the community in all root compartments. Whilst no selection of specific archaeal lineages within the root could be detected via sequencing, DGGE did indicate a possible shift in community composition across root compartments. The potential for interactions between soil AOA and plant roots remains largely unexplored. There is some limited evidence, however, which may indicate an influence of terrestrial plant root exudates on archaeal communities [81], and whilst the present work found no clear evidence that the total abundance of archaea changed within the rhizosphere, one study observed a negative correlation between archaeal abundance and plant root exudates [82]. There is also evidence that AOA can promote plant growth [34]. The nature of these interactions, however, still remains unclear. There is now mounting evidence that archaeal communities are influenced by plants or plant derived metabolites within the soil, even



if they do not utilise host derived carbon. In the future, longer read methods or metagenomics could be applied to better investigate archaeal community dynamics within the root microbiome.

*Burkholderiaceae*-family taxa (*Comamonadaceae* and *Oxalobacteriaceae*), and *Pseudomonadaceae* were identified as potential root exudate utilisers within the rhizosphere, in agreement with previous studies [42, 83]. These bacterial groups were also consistently enriched in the rhizosphere or endosphere, regardless of soil type. These results imply these families may be selectively recruited to the plants via root exudates, which support *Burkholderiaceae* and *Pseudomonadaceae* via photosynthetically fixed carbon. The *Pseudomonadaceae* family contains a diverse range of plant-beneficial and plant pathogenic strains [84, 85] but the literature correlates exudate utilisation with microbial functions which benefit the host plant [86, 87], and exudates can have a negative effect on plant pathogens [12]. While the mechanism of this selectivity remains unknown, it is likely these exudate utilisers are plant beneficial strains. Well studied representatives of this family with plant growth promoting traits include *Pseudomonas brassicaearum* [88] and *Pseudomonas fluorescens* [89]. Most of the exudate utilising families identified in the present work were fast growing Gram-negative bacteria. As observed by Worsley and colleagues (bioRxiv [90]), faster growing organisms are labelled more readily within a two-week incubation period. Due to their faster growth rates, these microorganisms can more easily monopolise the plant derived carbon within the rhizosphere and incorporate  $^{13}\text{C}$  into the DNA backbone during DNA replication. Slower growing organisms such as *Streptomycetaceae* are likely outcompeted for root derived resources in the rhizosphere or the two-week incubation period may be too short to allow the incorporation of the  $^{13}\text{C}$  label into DNA.

*Streptomycetaceae* were the most abundant of the core endosphere enriched families, despite not incorporating root derived carbon in the rhizosphere. This family is dominated by a single genus, *Streptomyces*. These filamentous Gram-positive bacteria are well known producers of antifungal and antibacterial secondary metabolites, and members of the genus have been shown to promote plant growth [79], have been correlated with increased drought tolerance [91], and can protect host plants from disease [78, 79]. *Streptomyces* species make up the active ingredients of horticultural products Actinovate and Mycostop and it has been proposed that plant roots may provide a major niche for these bacteria which are usually described as free-living, soil dwelling saprophytes. In this study *Streptomycetaceae* accounted for up to 40% of the bacteria present in the endosphere for some plants.

Intriguingly, after the plants senesced, there was a two-fold reduction in the abundance of *Streptomycetaceae* within the endosphere. This a surprising result for a bacterial group typically associated with the breakdown of dead organic matter within soils [92]. As plants senesce and die, a process of ecological succession occurs, where the tissues are colonised by different microbes (particularly fungi) successively as different resources within the plant tissues are degraded [93, 94]. The first microorganisms to colonise will be those rapidly metabolising sugars and lipids, followed later by more specialist organisms which will breakdown complex molecules like lignin and cellulose. While these later stages are typically attributed to fungi, *Streptomycetaceae* are known to degrade complex plant derived molecules such as hemicellulose and insoluble lignin [92, 95]. It could be that our sampling timepoint (late in the developmental senescence process, but prior to most biomass degradation) was too early in this succession process for any biomass fuelled *Streptomycetaceae* proliferation to be obvious. This, however, cannot explain the reduced abundance of *Streptomycetaceae* in senesced roots compared to the actively growing plants. This might be explained by a lack of active input from the plant, as the host senesces and resources are diverted to the developing grain [35] host derived resources may no longer be available to support *Streptomycetaceae* growth in the endosphere. The DNA-SIP experiment indicated that *Streptomycetaceae* did not utilise root exudates under the selected experimental conditions, which contradicts the findings of Ai and colleagues [43]. It must be noted that while *Streptomycetaceae* were not labelled in the DNA-SIP experiment, this experiment focused on the rhizosphere, and our data demonstrated that *Streptomycetaceae* primarily colonise the endosphere.

Further SIP experiments exploring the endosphere community, with more replicates to account for the high variability, may help to determine whether *Streptomycetaceae* can utilise plant derived carbon within the endosphere, and if the loss of these resources explains their reduced presence during senescence. Future studies should also investigate how *Streptomycetaceae* are able to colonise and survive within the endosphere of wheat. During developmental senescence, nitrogen is the main resource diverted to the developing grain [35]. It is possible that nitrogen, not carbon, is the resource provided by the host plant to support *Streptomycetaceae* growth. There is precedent for host-derived metabolites such as amino acids or gamma-aminobutyric acid (GABA) acting as a nitrogen source for root associated microbes [87, 96]. Additionally, there is evidence that the increased use

of nitrogen fertilizer (which correlates with greater total root exudation) was negatively correlated with the abundance of *Streptomyetaceae* in the rhizosphere [23]. In the future,  $^{15}\text{N}$ -nitrogen DNA or RNA-SIP could be used to explore whether *T. aestivum* var. Paragon is able to support *Streptomyetaceae* within the endosphere via nitrogen containing, host-derived metabolites. Lastly, it must be noted that the identification of core enriched taxa within the roots of *T. aestivum* var. Paragon cannot be extrapolated to other varieties of wheat; one study even suggests *T. aestivum* var. Paragon is an outlier amongst UK elite spring bread wheat with a particularly distinct microbiome [24]. To gain a more detailed understanding of which microbial taxa are associated with the roots of spring bread wheat, more genotypes must be analysed.

## Conclusions

In conclusion: (1) We identified five core microbial taxa associated within the rhizosphere and endosphere of *T. aestivum* var. Paragon, *Streptomyetaceae*, *Burkholderiaceae*, *Pseudomonadaceae*, *Rhizobiaceae* and *Chitinophagaceae*. The consistency of the enrichment of these groups across the soil types and plant growth stages we tested strongly indicates that they are core taxa associated with Paragon var. *T. aestivum*. (2) At the onset of developmental senescence, significant reductions in the abundance of many taxa were observed, including the whole core endosphere and rhizosphere microbiome, and multiple root-exudate utilising taxa. In particular, *Streptomyetaceae* abundance was reduced two-fold. This may indicate that active input from the host is required to maintain the abundance of certain families within the endosphere, and strongly indicated that this is the case for exudate utilisers. A significant increase in the total abundance of bacteria and archaea was evident during senescence and potentially increased colonisation of fungal groups associated with necrotrophy and plant tissue degradation. (3) No lineages of archaea were specifically associated with wheat roots. Conflicting data from DGGE and from 16S rRNA gene sequencing indicated that the currently available archaeal 16S rRNA gene databases are not sufficiently complete for this metabarcoding approach. (4) We identified nine taxa within the rhizosphere utilising carbon from wheat root exudates, including aforementioned core taxa of *T. aestivum* var. Paragon, *Pseudomonadaceae* and *Burkholderiaceae*. There was no evidence that the most abundant endosphere bacterial family *Streptomyetaceae* was using plant exudates within the rhizosphere. The present work has provided novel insights into the composition and variation within the wheat microbiome and how the community changes through developmental senescence.

Greater understanding is needed of the role played by the five core taxa associated with *T. aestivum* var. Paragon, and the mechanisms by which they are able to colonise the root and are supported by the host. This knowledge may inform novel agricultural applications or more ecologically responsible management strategies for wheat.

## Supplementary Information

The online version contains supplementary material available at <https://doi.org/10.1186/s40793-021-00381-2>.

**Additional file 1: Supplementary Figure 1.** Denaturing gel gradient electrophoresis (DGGE) showing archaeal 16S rRNA gene (A, B) or *amoA* (C, D) diversity across the bulk soil, rhizosphere and endosphere of wheat grown under laboratory conditions in agricultural soil (A, C) or Levington F2 compost (B, D). Primers are indicated in the Supplementary Table 6.

**Additional file 2: Supplementary Figure 2.** Denaturing gel gradient electrophoresis (DGGE) showing bacterial 16S rRNA gene diversity across the 12 fractions generated for stable isotope probing for the rhizosphere associated with the  $^{12}\text{C}$  control (top) and  $^{13}\text{C}$  labelled (top) plant ( $N=3$ ). Primers indicated in Supplementary Table 6.

**Additional file 3: Supplementary Figure 3.** Denaturing gel gradient electrophoresis (DGGE) showing archaeal 16S rRNA gene diversity across the 12 fractions generated for stable isotope probing for the rhizosphere associated with one  $^{12}\text{C}$  control (left) and  $^{13}\text{C}$  labelled (right) plant. Primers indicated in Supplementary Table 6.

**Additional file 4: Supplementary Figure 4.** Quantitative PCR against the fungal 18S rRNA gene to test for  $^{13}\text{C}$  labelling of the fungal community across fractions from the stable isotope probing. Graphs shows the percent of total 18S rRNA genes found within each of the 12 fractions for each plant (plotted as buoyant densities for that fraction in  $\text{g/ml}^{-1}$ ) for  $^{12}\text{C}$  control and  $^{13}\text{C}$  labelled wheat plants from rhizosphere (A) and endosphere compartments (B) ( $N=3$ ).

**Additional file 5: Supplementary Figure 5.** Endosphere stable isotope probing data. **A** Denaturing gel gradient electrophoresis (DGGE) showing bacterial 16S rRNA gene diversity across the 12 fractions generated for stable isotope probing for the endosphere associated with three  $^{12}\text{C}$  control (top) and  $^{13}\text{C}$  labelled (bottom) plants. These gels show a shift in the bacterial community towards the heavy fraction of  $^{13}\text{C}$  labelled plants. **B** Bars show the relative abundance of each bacterial group within the pooled sequenced  $^{12}\text{C}$  heavy,  $^{12}\text{C}$  light,  $^{13}\text{C}$  heavy and  $^{13}\text{C}$  light fractions ( $N=3$ ), for two separate sequencing runs on the same samples (old & new). **C** Principle coordinates analysis (PCoA) on bray curtis dissimilarities for the endosphere  $^{12}\text{C}$  heavy (orange/circle),  $^{12}\text{C}$  light (green/triangle),  $^{13}\text{C}$  heavy (blue/square) and  $^{13}\text{C}$  light (purple/cross) fractions ( $N=3$ ).

**Additional file 6: Supplementary Figure 6.** Denaturing gel gradient electrophoresis (DGGE) showing bacterial 16S rRNA gene diversity across the 12 fractions generated for stable isotope probing for the  $^{13}\text{C}$  unplanted soil controls ( $N=3$ ). Primers indicated in Supplementary Table 6.

**Additional file 7: Supplementary Table 1.** SIMPER outputs.

**Supplementary Table 2.** Permanova results. **Supplementary Table 3.** Soil chemical properties. **Supplementary Table 4.** SIP fractions used for sequencing. **Supplementary Table 5.** DESeq2 outputs to identify root exudate utilisers in the rhizosphere. **Supplementary Table 6.** Primers. **Supplementary Table 7.** PCR Conditions for metabarcoding, qPCR & DGGE PCRs. **Supplementary Table 8.** Qiime 2 Dada2 settings. **Supplementary Table 9.** Qiime2 taxonomy-based filtering stats. **Supplementary Table 10.** DESeq2 output identifying CO<sub>2</sub>-fixing autotrophs from unplanted soil. **Supplementary Table 11.** DESeq2 outputs stem elongation field grown- Significantly differentially abundant bacterial taxa. **Supplementary Table 12.** DESeq2 outputs (all pot grown and stem elongation)- Significantly differentially abundant bacteria.

**Supplementary Table 13.** DESeq2 outputs senescent plants- Significantly differentially abundant taxa. **Supplementary Table 14.** DESeq2 outputs stem elongation/senescent plants- Significantly differentially abundant bacterial taxa. **Supplementary Table 15.** DESeq2 outputs Significantly differentially abundant fungal taxa 01. **Supplementary Table 16.** DESeq2 outputs Significantly differentially abundant fungal taxa 02.

**Additional file 8: Supplementary Table 17.** Bacterial community composition data.

### Acknowledgements

S.M.M.P. and S.F.W. were funded by Natural Environment Research Council (NERC) PhD studentships (NERC Doctoral Training Programme grant NE/L002582/1). J.T.N. was funded by a Biotechnology and Biological Sciences Research Council (BBSRC) PhD studentship (BBSRC Doctoral Training Program grant BB/M011216/1). L.L.M. is supported by a Royal Society Dorothy Hodgkin Research Fellowship (DH150187) and by a European Research Council (ERC) Starting Grant (UNITY 852993). DNA sequencing was performed at Molecular Research Ltd. and we thank Dr. Scot E. Dowd for this service. Seed materials were acquired from the John Innes Centre Germplasm Resource Unit (JIC GRU) and we thank the whole GRU team for their invaluable support with this work. Field studies were performed at the John Innes Centre Field Studies Site in Bawburgh, and we thank the Simon Orford for invaluable help with field sampling, and the entire John Innes Centre Cereal Crop Research team for all their support. Computational analysis was performed using the High-Performance Computing Cluster supported by the Research and Specialist Computing Support service at the University of East Anglia and we would like to thank the entire team for their support with this work. We would like to thank Dr. Richard Oliver for valuable conversations on fungal taxonomy and fungal community dynamics during senescence.

### Authors' contributions

SMMP, JCM, LLM and MH designed the metabarcoding experiments and all authors contributed to the design of the stable isotope probing (SIP) experiment. SMMP performed all the metabarcoding and qPCR experiments, and SMMP and SFW performed all subsequent bioinformatic and statistical analysis. SP assessed the fungal and archaeal communities for the SIP experiment. SMMP and JTN performed the labelling, and the density gradient ultracentrifugation and fractionation for the SIP experiment. JTN performed bacterial community denaturing gradient gel electrophoresis, metabarcoding, and all subsequent bioinformatic and statistical analysis for the SIP experiment. Field sampling was performed by SMMP, JTN, and MH. All authors contributed to the development of and approved the final manuscript.

### Funding

This work was supported by the Natural Environment Research Council EnvEast/ARIES doctoral training partnership (NE/L002582/1), the Norwich Research Park BBSRC Doctoral Training Program (BB/M011216/1), a Royal Society Dorothy Hodgkin Research Fellowship (DH150187), by a European Research Council (ERC) Starting Grant (UNITY 852993), and by the Earth and Life Systems Alliance (ELSA) at the University of East Anglia.

### Availability of data and materials

The datasets generated during and/or analysed during the current study are available in the European Nucleotide Archive. Accession number PRJEB42686 (<https://www.ebi.ac.uk/ena/browser/view/PRJEB42686>).

### Declarations

#### Ethics approval and consent to participate

Not applicable.

#### Consent for publication

Not applicable.

#### Competing interests

The authors declare that they have no competing interests.

### Author details

<sup>1</sup>Department of Molecular Microbiology, John Innes Centre, Norwich Research Park, Norwich NR4 7UH, UK. <sup>2</sup>School of Biological Sciences, University of East Anglia, Norwich Research Park, Norwich NR4 7TJ, UK. <sup>3</sup>School of Environment, Earth & Ecosystem Sciences, The Open University, Milton Keynes MK7 6AA, UK. <sup>4</sup>School of Environmental Sciences, University of East Anglia, Norwich Research Park, Norwich NR4 7TJ, UK.

Received: 3 April 2021 Accepted: 13 May 2021

Published online: 21 June 2021

### References

- Borrill P, Harrington SA, Uauy C. Applying the latest advances in genomics and phenomics for trait discovery in polyploid wheat. *Plant J.* 2018;tpj.14150. <https://doi.org/10.1111/tpj.14150>.
- Loick N, Dixon ER, Abalos D, Vallejo A, Matthews GP, McGeough KL, et al. Denitrification as a source of nitric oxide emissions from incubated soil cores from a UK grassland soil. *Soil Biol Biochem.* 2016;95:1–7. <https://doi.org/10.1016/j.soilbio.2015.12.009>.
- Tilman D, Balzer C, Hill J, Befort BL. Global food demand and the sustainable intensification of agriculture. *Proc Natl Acad Sci.* 2011;108(50):20260–4. <https://doi.org/10.1073/pnas.1116437108>.
- Jog R, Pandya M, Nareshkumar G, Rajkumar S. Mechanism of phosphate solubilization and antifungal activity of *Streptomyces* spp isolated from wheat roots and rhizosphere and their application in improving plant growth. *Microbiology.* 2014;160(4):778–88. <https://doi.org/10.1099/mic.0.074146-0>.
- Palaniyandi SA, Damodharan K, Yang SH, Suh JW. *Streptomyces* sp. strain PGPA39 alleviates salt stress and promotes growth of 'micro tom' tomato plants. *J Appl Microbiol.* 2014;117(3):766–73. <https://doi.org/10.1111/jam.12563>.
- Bulgarelli D, Rott M, Schlaeppi K, Ver Loren van Themaat E, Ahmadinejad N, Assenza F, et al. Revealing structure and assembly cues for Arabidopsis root-inhabiting bacterial microbiota. *Nature.* 2012;488(7409):91–5. <https://doi.org/10.1038/nature11336>.
- Pascale A, Proietti S, Pantelides IS, Stringlis IA. Modulation of the root microbiome by plant molecules: the basis for targeted disease suppression and plant growth promotion. *Front Plant Sci.* 2020;10:1741. <https://doi.org/10.3389/fpls.2019.01741>.
- Iannucci A, Fragasso M, Beleggia R, Nigro F, Papa R. Evolution of the crop rhizosphere: impact of domestication on root exudates in tetraploid wheat (*Triticum turgidum* L.). *Front Plant Sci.* 2017;8:2124. <https://doi.org/10.3389/fpls.2017.02124>.
- Haichar Fel Z, Heulin T, Guyonnet JP, Achouak W. Stable isotope probing of carbon flow in the plant holobiont. *Curr Opin Biotechnol.* 2016;41:9–13. <https://doi.org/10.1016/j.copbio.2016.02.023>.
- Sasse J, Martinioia E, Northen T. Feed your friends: do plant exudates shape the root microbiome? *Trends Plant Sci.* 2018;23(1):25–41. <https://doi.org/10.1016/j.tplants.2017.09.003>.
- Bulgarelli D, Garrido-Oter R, Münch PC, Weiman A, Dröge J, Pan Y, et al. Structure and function of the bacterial root microbiota in wild and domesticated barley. *Cell Host Microbe.* 2015;17(3):392–403. <https://doi.org/10.1016/j.chom.2015.01.011>.
- Bais HP, Weir TL, Perry LG, Gilroy S, Vivanco JM. The role of root exudates in rhizosphere interactions with plants and other organisms. *Annu Rev Plant Biol.* 2006;57(1):233–66. <https://doi.org/10.1146/annurev.arplant.57.032905.105159>.
- Paul Chowdhury S, Babin D, Sandmann M, Jacquiod S, Sommermann L, Sørensen SJ, et al. Effect of long-term organic and mineral fertilization strategies on rhizosphere microbiota assemblage and performance of lettuce. *Environ Microbiol.* 2019;21(7):2426–39. <https://doi.org/10.1111/1462-2920.14631>.
- Bragina A, Berg C, Berg G. The core microbiome bonds the alpine bog vegetation to a transkingdom metacommunity. *Mol Ecol.* 2015;24(18):4795–807. <https://doi.org/10.1111/mec.13342>.
- Shade A, Handelsman J. Beyond the Venn diagram: the hunt for a core microbiome: the hunt for a core microbiome. *Environ Microbiol.* 2012;14(1):4–12. <https://doi.org/10.1111/j.1462-2920.2011.02585.x>.
- Lundberg DS, Lebeis SL, Paredes SH, Yourstone S, Gehring J, Malfatti S, et al. Defining the core *Arabidopsis thaliana* root microbiome. *Nature.* 2012;488(7409):86–90. <https://doi.org/10.1038/nature11237>.

17. Tian B, Zhang C, Ye Y, Wen J, Wu Y, Wang H, et al. Beneficial traits of bacterial endophytes belonging to the core communities of the tomato root microbiome. *Agric Ecosyst Environ*. 2017;247:149–56. <https://doi.org/10.1016/j.agee.2017.06.041>.
18. Yeoh YK, Paungfoo-Lonhienne C, Dennis PG, Robinson N, Ragan MA, Schmidt S, et al. The core root microbiome of sugarcane cultivated under varying nitrogen fertilizer application: N fertilizer and sugarcane root microbiota. *Environ Microbiol*. 2016;18(5):1338–51. <https://doi.org/10.1111/1462-2920.12925>.
19. Yeoh YK, Dennis PG, Paungfoo-Lonhienne C, Weber L, Brackin R, Ragan MA, et al. Evolutionary conservation of a core root microbiome across plant phyla along a tropical soil chronosequence. *Nat Commun*. 2017;8(1):215. <https://doi.org/10.1038/s41467-017-00262-8>.
20. Berg G, Smalla K. Plant species and soil type cooperatively shape the structure and function of microbial communities in the rhizosphere: plant species, soil type and rhizosphere communities. *FEMS Microbiol Ecol*. 2009;68(1):1–13. <https://doi.org/10.1111/j.1574-6941.2009.00654.x>.
21. Rascovan N, Carbonetto B, Perrig D, Díaz M, Canciani W, Abalo M, et al. Integrated analysis of root microbiomes of soybean and wheat from agricultural fields. *Sci Rep*. 2016;6(1):28084. <https://doi.org/10.1038/srep28084>.
22. Houlden A, Timms-Wilson TM, Day MJ, Bailey MJ. Influence of plant developmental stage on microbial community structure and activity in the rhizosphere of three field crops: plant and growth stage effects on microbial populations. *FEMS Microbiol Ecol*. 2008;65(2):193–201. <https://doi.org/10.1111/j.1574-6941.2008.00535.x>.
23. Chen S, Waghmode TR, Sun R, Kuramae EE, Hu C, Liu B. Root-associated microbiomes of wheat under the combined effect of plant development and nitrogen fertilization. *Microbiome*. 2019;7(1):136. <https://doi.org/10.1186/s40168-019-0750-2>.
24. Tkacz A, Pini F, Turner TR, Bestion E, Simmonds J, Howell P, et al. Agricultural selection of wheat has been shaped by plant-microbe interactions. *Front Microbiol*. 2020;11:132. <https://doi.org/10.3389/fmicb.2020.00132>.
25. Granzow S, Kaiser K, Wemheuer B, Pfeiffer B, Daniel R, Vidal S, et al. The effects of cropping regimes on fungal and bacterial communities of wheat and faba bean in a greenhouse pot experiment differ between plant species and compartment. *Front Microbiol*. 2017;8:902. <https://doi.org/10.3389/fmicb.2017.00902>.
26. Mavrodi DV, Mavrodi OV, Elbourne LDH, Tetu S, Bonsall RF, Parejko J, et al. Long-term irrigation affects the dynamics and activity of the wheat rhizosphere microbiome. *Front Plant Sci*. 2018;9:345. <https://doi.org/10.3389/fpls.2018.00345>.
27. Gdanetz K, Trail F. The wheat microbiome under four management strategies, and potential for endophytes in disease protection. *Phytobiomes*. 2017;1(3):158–68. <https://doi.org/10.1094/PBIOMES-05-17-0023-R>.
28. Kuźniar A, Włodarczyk K, Grządziel J, Goraj W, Gałązka A, Wolińska A. Culture-independent analysis of an endophytic core microbiome in two species of wheat: *Triticum aestivum* L. (cv. 'Hondia') and the first report of microbiota in *Triticum spelta* L. (cv. 'Rokosz'). *Syst Appl Microbiol*. 2020;43(1):126025. <https://doi.org/10.1016/j.syapm.2019.126025>.
29. Schlatter DC, Yin C, Hulbert S, Paulitz TC. Core rhizosphere microbiomes of dryland wheat are influenced by location and land use history. *Appl Environ Microbiol*. 2019;86:e02135–19. <https://doi.org/10.1128/AEM.02135-19>.
30. Turner TR, Ramakrishnan K, Walshaw J, Heavens D, Alston M, Swarbrick D, et al. Comparative metatranscriptomics reveals kingdom level changes in the rhizosphere microbiome of plants. *ISME J*. 2013;7(12):2248–58. <https://doi.org/10.1038/ismej.2013.119>.
31. Germida J, Siciliano S. Taxonomic diversity of bacteria associated with the roots of modern, recent and ancient wheat cultivars. *Biol Fertil Soils*. 2001;33(5):410–5. <https://doi.org/10.1007/s003740100343>.
32. Mahoney AK, Yin C, Hulbert SH. Community structure, species variation, and potential functions of rhizosphere-associated bacteria of different winter wheat (*Triticum aestivum*) cultivars. *Front Plant Sci*. 2017;8. <https://doi.org/10.3389/fpls.2017.00132>.
33. Baker GC, Smith JJ, Cowan DA. Review and re-analysis of domain-specific 16S primers. *J Microbiol Methods*. 2003;55(3):541–55. <https://doi.org/10.1016/j.mimet.2003.08.009>.
34. Song GC, Im H, Jung J, Lee S, Jung M, Rhee S, et al. Plant growth-promoting archaea trigger induced systemic resistance in *Arabidopsis thaliana* against *Pectobacterium carotovorum* and *Pseudomonas syringae*. *Environ Microbiol*. 2019;21(3):940–8. <https://doi.org/10.1111/1462-2920.14486>.
35. Distelfeld A, Avni R, Fischer AM. Senescence, nutrient remobilization, and yield in wheat and barley. *J Exp Bot*. 2014;65(14):3783–98. <https://doi.org/10.1093/jxb/ert477>.
36. Guiboileau A, Sormani R, Meyer C, Masclaux-Daubresse C. Senescence and death of plant organs: nutrient recycling and developmental regulation. *Comptes Rendus Biologies*. 2010;333(4):382–91. <https://doi.org/10.1016/j.crv.2010.01.016>.
37. Häffner E, Konietzki S, Diederichsen E. Keeping control: the role of senescence and development in plant pathogenesis and defense. *Plants*. 2015;4(3):449–88. <https://doi.org/10.3390/plants4030449>.
38. Zhalnina K, Louie KB, Hao Z, Mansoori N, da Rocha UN, Shi S, et al. Dynamic root exudate chemistry and microbial substrate preferences drive patterns in rhizosphere microbial community assembly. *Nat Microbiol*. 2018;3(4):470–80. <https://doi.org/10.1038/s41564-018-0129-3>.
39. Dumont MG, Murrell JC. Stable isotope probing — linking microbial identity to function. *Nat Rev Microbiol*. 2005;3(6):499–504. <https://doi.org/10.1038/nrmicro1162>.
40. Kong Y, Kuzyakov Y, Ruan Y, Zhang J, Wang T, Wang M, et al. DNA stable-isotope probing delineates carbon flows from rice residues into soil microbial communities depending on fertilization. *Appl Environ Microbiol*. 2020;86:e02151–19. <https://doi.org/10.1128/AEM.02151-19>.
41. Kaplan H, Ratering S, Felix-Henningsen P, Schnell S. Stability of in situ immobilization of trace metals with different amendments revealed by microbial 13C-labelled wheat root decomposition and efflux-mediated metal resistance of soil bacteria. *Sci Total Environ*. 2019;659:1082–9. <https://doi.org/10.1016/j.scitotenv.2018.12.441>.
42. Ai C, Liang G, Sun J, Wang X, He P, Zhou W, et al. Reduced dependence of rhizosphere microbiome on plant-derived carbon in 32-year long-term inorganic and organic fertilized soils. *Soil Biol Biochem*. 2015;80:70–8. <https://doi.org/10.1016/j.soilbio.2014.09.028>.
43. Uksa M, Buegger F, Gschwendtner S, Lueders T, Kublik S, Kautz T, et al. Bacteria utilizing plant-derived carbon in the rhizosphere of *Triticum aestivum* change in different depths of an arable soil: spatial distribution of rhizosphere bacteria. *Environ Microbiol Rep*. 2017;9(6):729–41. <https://doi.org/10.1111/1758-2229.12588>.
44. Donn S, Kirkegaard JA, Perera G, Richardson AE, Watt M. Evolution of bacterial communities in the wheat crop rhizosphere: rhizosphere bacteria in field-grown intensive wheat crops. *Environ Microbiol*. 2015;17(3):610–21. <https://doi.org/10.1111/1462-2920.12452>.
45. Kandeler E, Gerber H. Short-term assay of soil urease activity using colorimetric determination of ammonium. *Biol Fert Soils*. 1988;6(1). <https://doi.org/10.1007/BF00257924>.
46. Miranda KM, Espy MG, Wink DA. A rapid, simple spectrophotometric method for simultaneous detection of nitrate and nitrite 2001:10.
47. Neufeld JD, Vohra J, Dumont MG, Lueders T, Manefield M, Friedrich MW, et al. DNA stable-isotope probing. *Nat Protoc*. 2007;2(4):860–6. <https://doi.org/10.1038/nprot.2007.109>.
48. Bolyen E, Rideout JR, Dillon MR, Bokulich NA, Abnet CC, Al-Ghalith GA, et al. Reproducible, interactive, scalable and extensible microbiome data science using QIIME 2. *Nat Biotechnol*. 2019;37(8):852–7. <https://doi.org/10.1038/s41587-019-0209-9>.
49. Callahan BJ, McMurdie PJ, Rosen MJ, Han AW, Johnson AJA, Holmes SP. DADA2: high-resolution sample inference from Illumina amplicon data. *Nat Methods*. 2016;13(7):581–3. <https://doi.org/10.1038/nmeth.3869>.
50. Glöckner FO, Yilmaz P, Quast C, Gerken J, Beccati A, Ciuprina A, et al. 25 years of serving the community with ribosomal RNA gene reference databases and tools. *J Biotechnol*. 2017;261:169–76. <https://doi.org/10.1016/j.jbiotec.2017.06.1198>.
51. Nilsson RH, Larsson K-H, Taylor AFS, Bengtsson-Palme J, Jeppesen TS, Schigel D, et al. The UNITE database for molecular identification of fungi: handling dark taxa and parallel taxonomic classifications. *Nucleic Acids Res*. 2019;47(D1):D259–64. <https://doi.org/10.1093/nar/gky1022>.
52. Altschul SF, Gish W, Miller W, Myers EW, Lipman DJ. Basic Local Alignment Search Tool. n.d.;8. 1990.
53. R Core Team. R: a language and environment for statistical computing. Vienna: R Foundation for statistical computing; 2020.
54. Jari O, Blanchet FG, Friendly M, Roeland K, Legendre P, Minchin PR, et al. R package version 2.5–6. *Vegan: Community Ecology Package*; 2019.
55. Clarke KR. Non-parametric multivariate analyses of changes in community structure. *Austral Ecol*. 1993;18(1):117–43. <https://doi.org/10.1111/j.1442-9993.1993.tb00438.x>.

56. McMurdie PJ, Holmes S. phyloseq: An R package for reproducible interactive analysis and graphics of microbiome census data. *PLoS One*. 2013;8(4):e61217. <https://doi.org/10.1371/journal.pone.0061217>.
57. Ssekagiri A. microbiomeSeq: Microbial community analysis in an environmental context. R package version 0.1. 2020.
58. Dorn-In S, Bassitta R, Schwaiger K, Bauer J, Hölzel CS. Specific amplification of bacterial DNA by optimized so-called universal bacterial primers in samples rich of plant DNA. *J Microbiol Methods*. 2015;113:50–6.
59. Lehtovirta LE, Prosser JJ, Nicol GW. Soil pH regulates the abundance and diversity of group 1.1c Crenarchaeota. *FEMS Microbiol Ecol*. 2009;10:367–76.
60. Chemidlin Prévost-Bouré N, Christen R, Dequiedt S, Mougé C, Lelièvre M, Jolivet C, et al. Validation and application of a PCR primer set to quantify fungal communities in the soil environment by real-time quantitative PCR. *PLoS One*. 2011;6(9):e24166. <https://doi.org/10.1371/journal.pone.0024166>.
61. Lofgren LA, Uehling JK, Branco S, Bruns TD, Martin F, Kennedy PG. Genome-based estimates of fungal rDNA copy number variation across phylogenetic scales and ecological lifestyles. *Mol Ecol*. 2019;28(4):721–30. <https://doi.org/10.1111/mec.14995>.
62. Sun D-L, Jiang X, Wu QL, Zhou N-Y. Intragenomic heterogeneity of 16S rRNA genes causes overestimation of prokaryotic diversity. *Appl Environ Microbiol*. 2013;79(19):5962–9. <https://doi.org/10.1128/AEM.01282-13>.
63. Newitt JT, Prudence SMM, Hutchings MI, Worsley SF. Biocontrol of cereal crop diseases using Streptomyces. *Pathogens*. 2019;8(2):78. <https://doi.org/10.3390/pathogens8020078>.
64. Garbeva P, van Elsas JD, van Veen JA. Rhizosphere microbial community and its response to plant species and soil history. *Plant Soil*. 2008;302(1–2):19–32. <https://doi.org/10.1007/s11104-007-9432-0>.
65. Réblová M, Gams W, Seifert KA. Monilochaetes and allied genera of the Microascales. *Stud Mycol*. 2011;68:163–91. <https://doi.org/10.3114/sim.2011.68.07>.
66. Chen H, Ma Y, Zhang WF, Ma T, Wu HX. Molecular phylogeny of Colletotrichum (Sordariomycetes: Glomerellaceae) inferred from multiple gene sequences. *Genet Mol Res*. 2015;14(4):13649–62. <https://doi.org/10.4238/2015.October.28.27>.
67. Ghosh R, Bhadra S, Bandyopadhyay M. Department of Botany, University of Calcutta, 35 Ballygunge circular road, Kolkata, West Bengal, India. Morphological and molecular characterization of *Colletotrichum capsici* causing leaf-spot of soybean. *Trop Plant Res*. 2016;3(3):481–90. <https://doi.org/10.22271/tpr.2016.v3.i3.064>.
68. Zhang N, Castlebury LA, Miller AN, Huhndorf SM, Schoch CL, Seifert KA, et al. An overview of the systematics of the Sordariomycetes based on a four-gene phylogeny. *Mycologia*. 2006;98:1076–87.
69. Kowal J, Pressel S, Duckett JG, Bidartondo MI, Field KJ. From rhizoids to roots? Experimental evidence of mutualism between liverworts and ascomycete fungi. *Ann Bot*. 2018;121(2):221–7. <https://doi.org/10.1093/aob/mcx126>.
70. Midgley DJ, Greenfield P, Bissett A, Tran-Dinh N. First evidence of *Pezoloma ericae* in Australia: using the biomes of Australia soil environments (BASE) to explore the Australian phylogeography of known ericoid mycorrhizal and root-associated fungi. *Mycorrhiza*. 2017;27(6):587–94. <https://doi.org/10.1007/s00572-017-0769-9>.
71. Hambleton S, Sigler L. Meliniomyces, a new anamorph genus for root-associated fungi with phylogenetic affinities to *Rhizoscyphus ericae* (= *Hymenoscyphus ericae*), Leotiomycetes. *Stud Mycol*. 2005;53:1–27. <https://doi.org/10.3114/sim.53.1.1>.
72. Alves RJE, Minh BQ, Ulrich T, von Haeseler A, Schleper C. Unifying the global phylogeny and environmental distribution of ammonia-oxidising archaea based on amoA genes. *Nat Commun*. 2018;9(1):1517. <https://doi.org/10.1038/s41467-018-03861-1>.
73. Parks DH, Chuvochina M, Chaumeil P-A, Rinke C, Mussig AJ, Hugenholtz P. A complete domain-to-species taxonomy for Bacteria and archaea. *Nat Biotechnol*. 2020;38(9):1079–86. <https://doi.org/10.1038/s41587-020-0501-8>.
74. Fan K, Cardona C, Li Y, Shi Y, Xiang X, Shen C, et al. Rhizosphere-associated bacterial network structure and spatial distribution differ significantly from bulk soil in wheat crop fields. *Soil Biol Biochem*. 2017;113:275–84. <https://doi.org/10.1016/j.soilbio.2017.06.020>.
75. Fernández FA, Huhndorf SM. New species of *Chaetosphaeria*, *Melanopsammella* and *Tainosphaeria* gen. nov. from the Americas. *Fungal Diversity*. 2005;18:15–57.
76. Zhang Y, Crous PW, Schoch CL, Hyde KD. Pleosporales. *Fungal Divers*. 2012;53(1):1–221. <https://doi.org/10.1007/s13225-011-0117-x>.
77. Oliver R, Lichtenzveig J, Tan K-C, Waters O, Rybak K, Lawrence J, et al. Absence of detectable yield penalty associated with insensitivity to Pleosporales necrotrophic effectors in wheat grown in the west Australian wheat belt. *Plant Pathol*. 2014;63(5):1027–32. <https://doi.org/10.1111/ppa.12191>.
78. Shariffah-Muzaimah SA, Idris AS, Madiah AZ, Dzolkhifli O, Kamaruzzaman S, Maizatul-Suriza M. Characterization of Streptomyces spp. isolated from the rhizosphere of oil palm and evaluation of their ability to suppress basal stem rot disease in oil palm seedlings when applied as powder formulations in a glasshouse trial. *World J Microbiol Biotechnol*. 2018;34(1):15. <https://doi.org/10.1007/s11274-017-2396-1>.
79. Worsley SF, Newitt J, Rassbach J, Batey SFD, Holmes NA, Murrell JC, et al. Streptomyces endophytes promote host health and enhance growth across plant species. *Appl Environ Microbiol*. 2020;86:e01053–20. [/aem/86/16/AEM.01053-20.atom. https://doi.org/10.1128/AEM.01053-20](https://doi.org/10.1128/AEM.01053-20).
80. Carrión VJ, Cordovez V, Tyc O, Etalo DW, de Bruijn I, de Jager VCL, et al. Involvement of *Burkholderiaceae* and sulfurous volatiles in disease-suppressive soils. *ISME J*. 2018;12(9):2307–21. <https://doi.org/10.1038/s41396-018-0186-x>.
81. Sliwinski MK, Goodman RM. Comparison of Crenarchaeal consortia inhabiting the rhizosphere of diverse terrestrial plants with those in bulk soil in native environments. *Appl Environ Microbiol*. 2004;70(3):1821–6. <https://doi.org/10.1128/AEM.70.3.1821-1826.2004>.
82. Karlsson AE, Johansson T, Bengtson P. Archaeal abundance in relation to root and fungal exudation rates. *FEMS Microbiol Ecol*. 2012;80(2):305–11. <https://doi.org/10.1111/j.1574-6941.2012.01298.x>.
83. Macey MC, Pratscher J, Crombie AT, Murrell JC. Impact of plants on the diversity and activity of methylotrophs in soil. *Microbiome*. 2020;8(1):31. <https://doi.org/10.1186/s40168-020-00801-4>.
84. Mercado-Blanco J, Bakker PAHM. Interactions between plants and beneficial *Pseudomonas* spp.: exploiting bacterial traits for crop protection. *Antonie Van Leeuwenhoek*. 2007;92(4):367–89. <https://doi.org/10.1007/s10482-007-9167-1>.
85. Rico A, McCraw SL, Preston GM. The metabolic interface between *Pseudomonas syringae* and plant cells. *Curr Opin Microbiol*. 2011;14(1):31–8. <https://doi.org/10.1016/j.mib.2010.12.008>.
86. Chaparro JM, Badri DV, Bakker MG, Sugiyama A, Manter DK, Vivanco JM. Root exudation of phytochemicals in *Arabidopsis* follows specific patterns that are developmentally programmed and correlate with soil microbial functions. *PLoS One*. 2013;8(2):e55731. <https://doi.org/10.1371/journal.pone.0055731>.
87. Badri DV, Chaparro JM, Zhang R, Shen Q, Vivanco JM. Application of natural blends of phytochemicals derived from the root exudates of *Arabidopsis* to the soil reveal that phenolic-related compounds predominantly modulate the soil microbiome. *J Biol Chem*. 2013;288(7):4502–12. <https://doi.org/10.1074/jbc.M112.433300>.
88. Ortet P, Barakat M, Lalaouna D, Fochesato S, Barbe V, Vacherie B, et al. Complete genome sequence of a beneficial plant root-associated bacterium, *Pseudomonas brassicacearum*. *J Bacteriol*. 2013;193:3146.
89. Silby MW, Cerdeño-Tárraga AM, Vernikos GS, Giddens SR, Jackson RW, Preston GM, et al. Genomic and genetic analyses of diversity and plant interactions of *Pseudomonas fluorescens*. *Genome Biol*. 2009;10(5):R51. <https://doi.org/10.1186/gb-2009-10-5-r51>.
90. Worsley SF, Macey M, Prudence S, Wilkinson B, Murrell JC, Hutchings MI. Investigating the role of root exudates in recruiting *Streptomyces* bacteria to the *Arabidopsis thaliana* root microbiome. *Microbiology*. 2020. <https://doi.org/10.1101/2020.09.09.290742>.
91. Fitzpatrick CR, Copeland J, Wang PW, Guttman DS, Kotanen PM, Johnson MTJ. Assembly and ecological function of the root microbiome across angiosperm plant species. *Proc Natl Acad Sci U S A*. 2018;115(6):E1157–65. <https://doi.org/10.1073/pnas.1717617115>.
92. Chater KF, Biró S, Lee KJ, Palmer T, Schrepf H. The complex extracellular biology of *Streptomyces*. *FEMS Microbiol Rev*. 2010;34(2):171–98. <https://doi.org/10.1111/j.1574-6976.2009.02066.x>.
93. Carriás J-F, Gerphagnon M, Rodríguez-Pérez H, Borrel G, Loiseau C, Corbara B, et al. Resource availability drives bacterial succession during leaf-litter decomposition in a bromeliad ecosystem. *FEMS Microbiol Ecol*. 2020;96:fiaa045. <https://doi.org/10.1093/femsec/fiaa045>.
94. Purahong W, Wubet T, Lentendu G, Schloter M, Pecyna MJ, Kapturska D, et al. Life in leaf litter: novel insights into community dynamics of bacteria and fungi during litter decomposition. *Mol Ecol*. 2016;25(16):4059–74. <https://doi.org/10.1111/mec.13739>.

95. de Melo RR, Tomazetto G, Persinoti GF, Sato HH, Ruller R, Squina FM. Unraveling the cellulolytic and hemicellulolytic potential of two novel *Streptomyces* strains. *Ann Microbiol.* 2018;68(10):677–88. <https://doi.org/10.1007/s13213-018-1374-7>.
96. Moe LA. Amino acids in the rhizosphere: from plants to microbes. *Am J Bot.* 2013;100(9):1692–705. <https://doi.org/10.3732/ajb.1300033>.

### Publisher's Note

Springer Nature remains neutral with regard to jurisdictional claims in published maps and institutional affiliations.

**Ready to submit your research? Choose BMC and benefit from:**

- fast, convenient online submission
- thorough peer review by experienced researchers in your field
- rapid publication on acceptance
- support for research data, including large and complex data types
- gold Open Access which fosters wider collaboration and increased citations
- maximum visibility for your research: over 100M website views per year

**At BMC, research is always in progress.**

Learn more [biomedcentral.com/submissions](https://biomedcentral.com/submissions)

